

TIME-TERM ANALYSIS AND GEOLOGICAL INTERPRETATION OF SEISMIC TRAVEL-TIME DATA FROM THE COAST RANGES OF CENTRAL CALIFORNIA

BY ROBERT L. WESSON, JOHN C. ROLLER, AND W. H. K. LEE

ABSTRACT

Time terms resulting from an analysis of *P_g* seismic travel-time data from the Coast Ranges of central California yield a pattern that is remarkably consistent with other geological and geophysical estimates of depth to basement. A set of high-quality data for more than 330 paths was selected from all available travel-time observations from quarries and explosions. To assure a statistical estimate of the uncertainty of each time term, time terms were calculated only for sites recording arrivals from more than one source.

Time terms ranged from 0.0 to 1.5 sec, indicating depths to the *P_g* refractor of near-surface to more than 6 km, depending on assumed near-surface velocities. The *P_g* refractor is presumed to be granitic and metamorphic rocks southwest of the San Andreas Fault and volcanic or ultrabasic rocks within or beneath the Franciscan Formation northeast of the San Andreas Fault. Small time terms (< 0.4 sec) are associated with exposed granitic basement in the Santa Cruz and Gabilan ranges and with exposures of the Franciscan Formation in the central Diablo Range and in the Santa Teresa Hills (south of San Jose). Large time terms are associated with large thicknesses of upper Cretaceous and younger sedimentary rocks in the northern Santa Cruz Mountains, in the northern part of the Diablo Range, in structural troughs between the Zayante and San Andreas faults, and between the Sargent and San Andreas faults and in the Hollister Trough. Time terms for sites athwart structural discontinuities, particularly the San Andreas Fault, vary with the direction of the approaching ray. Time terms for sites on the relatively homogeneous granitic mass of the Gabilan Range increase with elevation.

The large differences in magnitude of these time terms and the nature of the distribution clearly demonstrate that the laterally inhomogeneous Earth's crust in this area must be taken into account in the location of local earthquakes where high accuracy is required. These time terms provide a firm basis for the necessary station corrections.

INTRODUCTION

A time-term analysis of the seismic travel-time data from the Coast Ranges of central California was undertaken to improve understanding of the distribution of seismic wave velocities in the upper crust and its relation to geological structure and to obtain seismograph station time corrections for improving the location of local earthquakes.

The surficial geology of the Coast Ranges of central California, here taken to include the Santa Cruz, Diablo, and Gabilan ranges between approximately 36° and 38°N latitude, is dominated by lateral discontinuities across the San Andreas, Hayward, and Calaveras faults (Figure 1). West of the Pilarcitos and San Andreas faults, the basement is thought to be composed of a complex of granitic and metamorphic rocks. East of the

Pilarcitos and San Andreas faults, crystalline basement is not exposed within the area discussed here nor has it been penetrated by drilling. The oldest exposed rocks are those of the Franciscan Formation, a complex eugeosynclinal assemblage of greywackes, cherts, and volcanic and ultramafic rocks. It is probable that these rocks are underlain by basaltic or ultramafic rocks (Bailey *et al.*, 1964). In this paper, "basement" is broadly taken to mean the geological unit that acts as a refractor for the seismic phase, P_g , which has a velocity of about 6.0 km/sec and is the first seismic wave from surface sources to arrive at stations approximately 25 to 70 km distant. The basement rocks are deeply buried by sedimentary rocks over a large part of the area, particularly in the valleys east of the San Andreas Fault and locally within the mountains. Recent reviews of California coast range geology may be found in Page (1966) and Bailey *et al.* (1964).

Byerly (1939) made the first systematic seismic refraction studies in the area, using both earthquakes and explosions. The velocity 5.61 km/sec he obtained for P_g was exclusively for travel paths on the northeast side of the San Andreas Fault. Healy (1963) obtained a velocity of 6.1 km for travel paths southwest of the fault. Eaton (1963) analyzed data from a profile extending to the northeast from San Francisco. As the profile was perpendicular to the structural trend, the P_g velocity could not be reliably determined, but the results were consistent with a velocity of about 6.0 km/sec. Hamilton *et al.* (1964) obtained a velocity of 6.28 km/sec on the southwest side of the fault for a profile northwest from a quarry (Q03 in this paper) near Salinas. Turcotte (1964) used a velocity of 6.0 km for the Hollister area based on travel times from Q03 and the work of Healy to calculate delay times in the Hollister area. Stewart (1968) gave results of detailed, reversed profiles in the Diablo and Gabilan ranges on both sides of the fault and obtained velocities of 5.7 km/sec for the northeast side and 6.1 km/sec for the southwest side.

Mikumo (1965), Otsuka (1966a, b), McEvelly (1966) and Kind (1972) have used data from seismograph arrays, mostly from sources at teleseismic or regional distances, to estimate crustal structure in this area. Their results generally show a thickening of the crust to the east away from the continental margin.

The time-term method assumes that the travel time, T_{ij} , from i th source to the j th station may be represented in the form

$$T_{ij} = \frac{\Delta_{ij}}{v_{\text{ref}}} + a_i + a_j + r_{ij}$$

where Δ_{ij} is the distance from the i th source to the j th station, v_{ref} is the velocity of refracting horizon, a_i and a_j are the time terms, and r_{ij} is the residual.

The time terms are related to the depth, h , to the refractor, and to the velocity distribution, $v(z)$, above it, by the relation

$$a_i = \int_0^{h_i} \frac{[v_{\text{ref}}^2 - v^2(z)]^{1/2} dz}{v_{\text{ref}} v(z)}$$

(Berry and West, 1966a). For the simple case $v(z) = v$, a constant,

$$a_i = h_i \cos \theta / v,$$

where

$$\cos \theta = (v_{\text{ref}}^2 - v^2)^{1/2} / v_{\text{ref}}.$$

The resulting system of equations may be solved for the a_i and a_j by least squares, minimizing the sum of squares of the r_{ij} . The velocity v_{ref} may be held fixed, or may be obtained from the solution.

The time-term technique is particularly suited to the interpretation of travel-time data in this geological situation because it can delineate the main sources of inhomogeneity expected, the variation in depth to basement and of near-surface velocities. Station corrections for earthquake location can then be derived from the time terms. Circumstances that could adversely affect the time-term technique are lateral changes in the basement velocity and the presence of large strike-slip faults that might separate crustal blocks with substantially different basement velocities. The geological assumptions are that the refractor velocity is constant in the area of consideration and that in the vicinity of each site the basement relief and the lateral variation in the velocity above the refractor are small enough that time terms calculated from various azimuths will be approximately the same. These conditions are not always met in this area. The applicability of the method and the required modifications in specific situations are discussed below. The fundamentals of the time-term method have been discussed by many workers, notably Scheidegger and Willmore (1957), Willmore and Bancroft (1960), and Berry and West (1966a, b). Hamilton (1970) gives a recent example of the application of the time-term method to the problem of deriving station corrections for earthquake location.

DATA ACQUISITION AND ANALYSIS

Travel-time data for the Coast Ranges of central California have been collected in various ways: at permanent seismograph stations recording on paper records, 16-mm film, and magnetic tape, and at portable seismograph stations recording on magnetic tape and with truck-mounted systems especially designed for crustal refraction studies. All available travel-time data were evaluated, with emphasis on that collected by the U.S. Geological Survey, in order to extract that fraction that is of high quality and is sufficiently redundant to allow some statistical measure of the reliability of the time terms derived from it. The sources and recording sites for the complete data are shown on Figure 1, and their designations, coordinates, and elevations are given in Table 1.

Recordings at seismograph stations of the U.S. Geological Survey telemeter network (Eaton *et al.*, 1970) constituted the bulk of the observations. Arrival times recorded at these stations are routinely measured to the nearest 0.05 sec. For some critical data, high-speed playbacks were made and times could then be determined to the nearest 0.01 sec. Times from the portable seismographs can be read to 0.03 sec.

Recordings from quarry blasts constituted most of the data (Table 1) obtained from the permanent network. Several blasts were recorded from most of the quarries. Except for quarries, Q06 and Q07, the shot time for at least one of the shots was determined to 0.01 sec by recording at the quarry. The travel time to the nearest permanent station was then used to calculate other shot times.

Where a station recorded numerous explosions from a quarry, the observations were statistically analyzed. First, the mean travel time and standard deviation were calculated; then, all observations that differed from the mean by more than one standard deviation were eliminated; finally, the mean was recalculated. This process eliminated gross identification and timing errors and smoothed the minor effects of errors in timing and small changes in blast location. The number of observations and the standard errors are listed with the mean travel times in Table 2.

Additional data were obtained from two 2,000-lb explosions fired by the U.S. Geological Survey, one south of San Jose (SPSJ) and the other near Hollister (SPHL). Nineteen portable stations and seven truck-mounted seismic refraction systems were operated in the vicinity of the Sargent Fault to record these shots. The shots were also recorded by the permanent network.

TABLE 1

DESIGNATIONS, COORDINATES, AND ELEVATIONS FOR ALL SITES CONTRIBUTING TRAVEL-TIME DATA

Table 1				PTV 36 6.45 120 43.25 533				18L1 37 16.66 121 27.25 707										
USGS QUARRY DATA				PVR 37 25.75 121 15.52 159				18L2 37 16.66 121 27.50 621										
SITE	LAT(N)	LONG(W)	ELEV(M)	T.T.	SITE	LAT(N)	LONG(W)	ELEV(M)	T.T.	SITE	LAT(N)	LONG(W)	ELEV(M)	T.T.				
Q00	37	14.65	121	52.10	70	*												
Q03	36	45.06	121	35.88	177	*												
Q04	36	54.38	121	37.38	40	*												
Q05	37	19.37	122	6.75	550	*												
Q06	37	29.70	122	23.74	110	*												
Q07	37	32.12	122	4.35	10	*												
Q08	37	42.92	122	21.78	4	*												
Q09	36	47.50	121	28.45	300	*												
Q10	37	2.86	122	10.67	300	*												
USGS SHOT DATA				USGS TRUCKS AND PORTABLE STATIONS														
SITE	LAT(N)	LONG(W)	ELEV(M)	T.T.	SITE	LAT(N)	LONG(W)	ELEV(M)	T.T.	SITE	LAT(N)	LONG(W)	ELEV(M)	T.T.				
SPS3	37	11.88	121	45.50	0	*	H-1	37	11.63	121	45.55	99						
SPHL	36	49.53	121	19.32	0	*	H-2	37	11.76	121	45.68	96						
SHOT POINTS (STEWART,1968)																		
SITE	LAT(N)	LONG(W)	ELEV(M)	T.T.	J-1	37	5.17	121	42.88	158								
BBN1	37	13.36	122	13.75	536					J-2	37	4.98	121	42.68	171			
BBN2	37	13.48	122	13.71	548	*	J-3	37	4.77	121	42.52	158						
SJM	36	46.10	121	34.50	109	*	J-4	37	4.62	121	42.32	145						
GNZ	36	31.36	121	17.85	609	*	J-5	37	4.43	121	42.10	152						
HRN	36	17.90	120	59.20	259	*	J-6	37	4.16	121	42.08	166	*					
RAN	35	52.70	120	35.53	420	*	K-2	37	1.70	122	39.35	91	*					
PAN	36	39.00	120	49.60	487	*	P-1	36	49.65	121	20.13	165						
PCH	37	2.05	121	8.69	158	*	P-2	36	49.63	121	20.47	158						
MTS	37	17.33	121	27.42	670	*	P-3	36	49.83	121	20.63	154						
CED	37	34.07	121	34.93	594	*	P-4	36	49.93	121	20.93	147						
BEH	38	4.75	122	10.20	109	*	P-5	36	49.92	121	21.27	143						
							P-6	36	49.93	121	21.62	133						
SHOT POINTS (EATON,UNPUBLISHED DATA)																		
SITE	LAT(N)	LONG(W)	ELEV(M)	T.T.	Q-1	36	53.58	121	28.50	79								
BVSP	36	33.91	121	12.71	549	*	Q-2	36	53.35	121	28.39	76						
PESP	36	55.05	121	35.72	64	*	Q-3	36	53.11	121	28.25	89						
							Q-4	36	52.86	121	28.14	85						
NATIVIDAD QUARRY (TURCOTTE,1964)																		
SITE	LAT(N)	LONG(W)	ELEV(M)	T.T.	Q-5	36	52.57	121	28.09	98								
Q031	36	45.20	121	35.60	0		J-6	36	52.32	121	28.16	93						
Q032	36	45.10	121	35.60	0		S-1	37	9.43	121	44.89	207						
Q033	36	44.90	121	35.50	0		S-2	37	9.16	121	44.87	194						
Q034	36	45.00	121	35.50	0		S-3	37	9.03	121	44.67	195						
Q035	36	45.20	121	35.60	0		S-4	37	8.88	121	44.33	181						
Q036	36	45.00	121	35.50	0		S-5	37	8.64	121	44.18	189						
Q037	36	45.00	121	35.80	0		S-6	37	8.37	121	44.07	171						
Q038	36	45.00	121	35.70	0		T-1	36	49.65	121	19.96	174						
Q039	36	45.00	121	35.50	0		T-2	36	49.47	121	19.68	195						
Q310	36	45.20	121	35.60	0		T-3	36	49.45	121	19.45	207						
Q311	36	45.06	121	35.60	0		S01	37	9.44	121	50.83	204						
Q312	36	45.00	121	35.50	0		S02	37	4.00	121	56.90	98	*					
							S03	37	4.63	121	50.34	523	*					
							S04	37	1.60	121	46.18	219	*					
							S05	36	58.38	121	38.91	393						
							S06	37	57.62	121	37.58	215						
							S07	36	56.24	121	34.17	95	*					
							S08	36	55.36	121	38.35	277	*					
							S09	36	58.85	121	47.12	108	*					
							S10	37	1.73	121	50.55	329	*					
							S11	37	5.57	121	44.56	206	*					
							S12	37	2.13	121	40.79	146	*					
							S13	37	0.34	121	42.60	486	*					
							S14	37	0.22	121	38.30	171	*					
							S15	36	53.11	121	35.50	121	*					
							S16	37	8.44	121	56.91	268	*					
							S17	36	46.44	121	14.38	320	*					
							S18	37	6.53	121	28.67	361	*					
YANKEE SHOT POINT (HEALY,1963)								DIABLO STATIONS (STEWART,1968)										
SITE	LAT(N)	LONG(W)	ELEV(M)	T.T.	SITE	LAT(N)	LONG(W)	ELEV(M)	T.T.	ENGL	36	46.87	121	0.56	609			
YANK	37	36.08	122	41.55	0		1K3	38	17.87	122	22.93	109	ENGL2	36	47.17	121	0.95	994
							1K6	38	17.37	122	22.48	91	ENGL3	36	47.14	121	0.11	624
							2H1	38	4.72	122	10.17	103	WISE	36	48.89	120	57.49	518
							4J1	37	48.07	121	46.95	585	ORTI	36	47.12	120	55.74	1036
							4J6	37	47.13	121	46.20	579	NINE	36	45.38	120	53.98	381
							S01	37	37.60	121	42.20	228	VASQ	36	42.75	120	54.38	472
							S06	37	36.50	121	41.53	377	CER1	36	43.60	120	58.14	1021
							651	37	35.57	121	37.62	556	CER2	36	43.32	120	57.77	1051
							656	37	35.28	121	36.22	615	CER3	36	43.32	120	57.77	1051
							7T1	37	34.49	121	35.17	624	VALL1	36	27.73	120	39.98	963
							7T6	37	33.65	121	34.76	624	VALL2	36	27.63	120	39.43	655
							8P1	37	33.10	121	34.28	358	VALL3	36	27.38	120	39.03	678
							8P6	37	32.02	121	33.63	670						
							9R1	37	31.66	121	33.28	373						
							9R6	37	30.65	121	32.36	501						
							7M1	37	34.46	121	35.18	797						
							7M3	37	34.17	121	34.90	627						
							2M1	38	4.09	122	10.10	60						
							2M3	38	4.59	122	9.95	121						
							10J1	37	29.92	121	32.15	713						
							10J6	37	28.80	121	31.70	792						
							11K1	37	28.45	121	31.45	792						
							11K6	37	27.22	121	30.90	838						
							12R1	37	26.80	121	31.03	862						
							12R6	37	25.80	121	30.52	499						
							13H1	37	25.09	121	30.10	792						
							13H6	37	24.15	121	29.60	624						
							14Q1	37	23.77	121	29.35	658						
							14Q6	37	22.30	121	28.98	621						
							15S1	37	21.30	121	28.70	630						
							15S6	37	20.05	121	28.50	630						
							16T1	37	19.58	121	28.45	633						
							16T6	37	18.42	121	27.90	646						
							17P1	37	17.96	121	27.61	658						
							17P6	37	16.95	121	27.40	548						

TABLE 2

SHOT AND STATION DESIGNATIONS, DISTANCES AND TRAVEL TIMES FOR TRAVEL PATHS EXAMINED IN THIS

STUDY

Table 2						SHOT SITE DELTA N T S.D. SOLN						SHOT SITE DELTA N T S.D. SOLN																																											
USGS PIAZZA PAVING						005 PEM 0.66 2 0.37 0.05	009 JHC 28.13 18 5.21 0.02	009 PNC 29.30 28 5.12 0.02	009 S13 31.71 2 7.20 0.24	009 S18 35.20 1 7.78 0.00	009 CBO 40.34 1 8.58 0.00	009 S10 42.07 2 8.78 0.07	009 AND 43.25 1 8.98 0.00	009 SPG 46.34 9 8.15 0.04	009 ALM 52.51 110.63 0.00	009 COE 54.65 212.03 0.07	009 ARN 62.11 112.18 0.00	009 MHR 67.82 115.68 0.00	009 PWR 74.66 114.88 0.00	009 JCL 83.19 115.53 0.00																																			
000 SWC 9.64 2 2.45 0.11	000 ALM 9.71 1 2.38 0.00	000 MHR 16.20 2 4.13 0.00	000 COE 17.43 2 4.38 0.14	000 CBO 21.67 2 4.65 0.04	000 PWR 23.37 2 5.33 0.07	000 ALM 23.78 1 5.33 0.00	000 POR 30.64 1 6.78 0.00	USGS KAISER-NATIVIDAD						USGS PCA-DAVENPORT																																									
USGS KAISER-NATIVIDAD						005 SFT 10.72 16 3.10 0.03	005 POR 11.08 16 2.87 0.00	005 LHD 14.91 4 3.57 0.00	005 MOB 15.46 3 4.09 0.03	005 WDS 17.65 14 4.12 0.05	005 BCR 19.51 20 4.44 0.05	005 BCU 20.18 2 4.77 0.00	005 S16 24.92 3 4.57 0.03	005 CYH 26.26 16 5.68 0.02	005 ALM 29.82 17 6.08 0.04	005 SOI 29.87 2 6.05 0.04	005 SVC 30.44 12 6.95 0.04	005 CAL 31.15 14 6.57 0.03	005 MHR 31.84 24 7.22 0.04	005 S02 31.95 1 1.42 0.00	005 EGR 31.99 3 6.24 0.03	005 PVR 34.83 3 7.74 0.00	005 S03 36.51 3 7.07 0.00	005 PAL 36.92 17 7.89 0.02	005 SAL 39.33 3 7.77 0.05	005 COE 39.68 9 8.73 0.05	005 S11 41.55 4 8.02 0.07	005 CBO 44.31 1 8.67 0.00	005 AND 46.87 4 9.52 0.00	005 S12 49.82 2 9.27 0.00	005 S13 50.16 1 8.87 0.00	005 ARN 51.50 210.19 0.04	005 BCL 54.94 211.15 0.04	005 S14 55.02 110.47 0.00	005 ANG 66.00 312.70 0.03	005 PCL 78.96 314.57 0.05	005 S15 86.43 115.67 0.00	005 PNC 94.48 117.17 0.00	005 QSR 96.77 117.97 0.00	USGS PCA-PILARCITOS															
003 SJG 5.71 1 1.25 0.00	003 STL 10.22 13 2.26 0.02	003 SRS 11.57 10 2.45 0.03	003 FDR 13.98 5 2.80 0.01	003 ANZ 14.85 7 3.05 0.01	003 S08 19.40 2 3.99 0.08	003 DCR 20.13 2 4.74 0.08	003 CBC 20.76 2 4.69 0.13	003 SC7 20.84 1 4.70 0.00	003 PNC 21.23 10 4.23 0.02	003 CHR 23.10 8 4.95 0.01	003 CNR 23.23 7 4.37 0.02	003 S06 23.37 1 4.98 0.00	003 FMR 24.04 3 5.26 0.04	003 HCC 27.87 2 6.10 0.07	003 S14 28.27 1 5.58 0.00	003 JHC 29.19 9 5.49 0.03	003 S15 29.83 1 6.48 0.00	003 S13 29.57 1 5.90 0.00	003 S09 30.48 1 6.65 0.00	003 S17 32.08 2 6.74 0.01	003 CAN 32.10 3 6.64 0.01	003 S12 32.40 2 6.19 0.01	003 S04 34.21 1 7.08 0.00	003 STC 35.10 3 6.71 0.10	003 OSR 35.67 4 7.24 0.01	003 S10 37.76 2 7.52 0.02	003 EUC 38.23 3 7.71 0.13	003 S11 40.07 1 7.55 0.00	003 CBO 40.85 2 7.75 0.00	003 S18 41.13 1 8.28 0.00	003 S03 42.05 1 7.93 0.00	003 PCL 43.25 5 8.65 0.03	003 AND 45.71 2 8.77 0.11	003 S02 46.93 1 8.58 0.00	003 SFG 48.47 8 8.59 0.02	003 SLD 49.22 210.24 0.06	003 ALM 50.35 1 5.35 0.00	003 COE 56.62 211.25 0.00	003 LRV 63.13 211.55 0.00	003 CRC 72.18 114.15 0.00	003 HER 81.41 214.61 0.26	003 JCL 83.44 114.78 0.00	USGS GRANITE ROCK-LOGAN												
USGS GRANITE ROCK-LOGAN						007 SFT 17.09 4 3.26 0.05	007 WDS 21.94 5 4.16 0.04	007 LTN 23.29 4 4.35 0.06	007 CAL 25.91 6 4.78 0.03	007 BOL 31.18 5 5.83 0.05	007 SCL 31.31 4 5.59 0.05	007 PVR 31.47 1 5.90 0.00	007 PDR 32.63 6 6.07 0.03	007 MHR 34.12 2 6.30 0.07	007 ALM 46.37 5 8.13 0.03	007 COE 46.95 2 8.90 0.07	007 ANG 47.97 3 8.32 0.03	USGS U.S.NAVY-HUNTERS POINT																																					
004 ANZ 3.74 1 0.90 0.00	004 S07 5.88 1 2.00 0.00	004 S06 6.00 2 1.80 0.07	004 CPH 6.76 6 2.08 0.03	004 SCS 7.74 2 2.13 0.04	004 CIL 8.10 6 1.98 0.03	004 FMR 8.26 9 2.18 0.04	004 OCR 10.35 1 3.00 0.00	004 S14 10.89 2 2.57 0.18	004 HCC 12.16 2 2.90 0.14	004 SUG 12.76 8 2.80 0.03	004 S13 13.47 2 3.32 0.18	004 S12 15.20 2 3.40 0.07	004 S09 16.66 2 4.18 0.11	004 CAN 18.12 5 4.35 0.00	004 S04 18.68 2 4.82 0.11	004 FDR 19.77 1 5.50 0.00	004 FUC 23.06 2 5.38 0.11	004 S10 23.80 2 5.50 0.07	004 S18 25.92 2 5.68 0.11	004 S03 27.00 1 5.75 0.00	004 SRS 27.98 3 5.22 0.04	004 S15 28.16 2 6.52 0.04	004 AND 28.41 3 5.98 0.03	004 CNR 33.20 2 7.95 0.07	004 PCL 33.77 4 7.14 0.07	004 ALM 34.35 2 7.07 0.04	004 S17 37.23 1 6.95 0.00	004 QSR 37.55 3 8.00 0.00	004 PNC 38.21 2 7.02 0.04	004 S16 38.93 1 7.90 0.00	004 COE 39.24 2 8.55 0.00	004 SVC 44.00 2 9.05 0.07	004 JHC 44.90 1 8.00 0.00	004 STC 46.12 1 9.50 0.00	004 ARN 49.82 210.02 0.04	004 CRC 58.47 110.60 0.00	004 CAL 62.45 112.20 0.00	004 SHG 63.85 113.45 0.00	004 MNR 76.40 115.60 0.00	USGS KAISER-PERMANETE															
USGS KAISER-PERMANETE						009 SRS 14.24 31 2.86 0.02	009 EGR 14.24 2 3.95 0.04	009 ANZ 14.66 19 3.23 0.04	009 CNR 14.84 35 3.18 0.04	009 DIL 15.01 28 3.58 0.04	009 S15 18.07 7 4.82 0.13	009 CHR 21.00 4 5.09 0.02	009 S17 21.02 5 5.22 0.16	009 QSR 23.88 22 5.67 0.03	009 CAN 25.93 1 6.18 0.00	009 S16 28.13 18 5.21 0.02	009 PNC 29.30 28 5.12 0.02	009 S13 31.71 2 7.20 0.24	009 S18 35.20 1 7.78 0.00	009 CBO 40.34 1 8.58 0.00	009 S10 42.07 2 8.78 0.07	009 AND 43.25 1 8.98 0.00	009 SPG 46.34 9 8.15 0.04	009 ALM 52.51 110.63 0.00	009 COE 54.65 212.03 0.07	009 ARN 62.11 112.18 0.00	009 MHR 67.82 115.68 0.00	009 PWR 74.66 114.88 0.00	009 JCL 83.19 115.53 0.00	010 FGR 6.68 1 1.52 0.00	010 BCR 18.45 16 4.12 0.06	010 S02 20.51 2 3.90 0.04	010 S16 22.85 2 4.80 0.00	010 PDR 24.15 13 5.20 0.08	010 STV 26.72 15 5.54 0.09	010 S03 30.30 2 5.95 0.00	010 ALM 31.87 12 6.03 0.08	010 EUC 32.82 2 6.67 0.14	010 LTN 34.04 14 6.78 0.10	010 SFT 39.67 1 7.87 0.00	010 CBO 44.05 1 8.47 0.00	010 FMR 44.24 2 8.80 0.04	010 DIL 53.10 2 9.80 0.00	010 CHR 53.71 3 9.90 0.03	010 ANZ 55.29 1 6.82 0.00	010 SJG 60.56 311.02 0.00	010 CAN 61.87 1 9.02 0.00	010 SRS 72.25 1 8.57 0.00	010 PNC 72.38 1 8.17 0.00	USGS HOLLISTER SHOT					
USGS HOLLISTER SHOT						008 SAL 16.36 1 3.50 0.00	008 ANG 17.23 4 3.52 0.03	008 BOL 28.77 3 5.90 0.00	008 CYS 29.44 7 5.65 0.04	008 MHR 33.96 5 6.73 0.05	008 PAL 37.07 7 7.40 0.00	008 SFT 38.19 1 7.55 0.00	008 CAL 57.78 110.60 0.00	008 SMC 70.76 114.10 0.00	008 ALM 76.87 113.70 0.00	008 COE 79.42 114.80 0.00	008 CBO 89.72 116.40 0.00	008 S12 39.50 7.84	008 HCC 39.67 8.54	008 S13 39.95 8.18	008 PNC 40.54 8.14	008 J-6 43.31 8.46	008 J-5 43.64 8.60	008 J-4 44.08 8.65	008 J-2 44.92 8.77	008 S09 44.75 8.64	008 J-1 45.37 8.85	008 S04 45.73 9.54	008 CBO 45.57 9.59	008 SHG 46.05 9.19	008 S11 47.78 9.16	008 S-6 50.62 9.76	USGS SLACKEVINNING-DUMBARTON																						
USGS SLACKEVINNING-DUMBARTON						007 SFT 17.09 4 3.26 0.05	007 WDS 21.94 5 4.16 0.04	007 LTN 23.29 4 4.35 0.06	007 CAL 25.91 6 4.78 0.03	007 BOL 31.18 5 5.83 0.05	007 SCL 31.31 4 5.59 0.05	007 PVR 31.47 1 5.90 0.00	007 PDR 32.63 6 6.07 0.03	007 MHR 34.12 2 6.30 0.07	007 ALM 46.37 5 8.13 0.03	007 COE 46.95 2 8.90 0.07	007 ANG 47.97 3 8.32 0.03	008 S12 39.50 7.84	008 HCC 39.67 8.54	008 S13 39.95 8.18	008 PNC 40.54 8.14	008 J-6 43.31 8.46	008 J-5 43.64 8.60	008 J-4 44.08 8.65	008 J-2 44.92 8.77	008 S09 44.75 8.64	008 J-1 45.37 8.85	008 S04 45.73 9.54	008 CBO 45.57 9.59	008 SHG 46.05 9.19	008 S11 47.78 9.16	USGS IDEAL CEMENT-S.J.BAUTISTA																							
USGS IDEAL CEMENT-S.J.BAUTISTA						009 SRS 14.24 31 2.86 0.02	009 EGR 14.24 2 3.95 0.04	009 ANZ 14.66 19 3.23 0.04	009 CNR 14.84 35 3.18 0.04	009 DIL 15.01 28 3.58 0.04	009 S15 18.07 7 4.82 0.13	009 CHR 21.00 4 5.09 0.02	009 S17 21.02 5 5.22 0.16	009 QSR 23.88 22 5.67 0.03	009 CAN 25.93 1 6.18 0.00	009 S16 28.13 18 5.21 0.02	009 PNC 29.30 28 5.12 0.02	009 S13 31.71 2 7.20 0.24	009 S18 35.20 1 7.78 0.00	009 CBO 40.34 1 8.58 0.00	009 S10 42.07 2 8.78 0.07	009 AND 43.25 1 8.98 0.00	009 SPG 46.34 9 8.15 0.04	009 ALM 52.51 110.63 0.00	009 COE 54.65 212.03 0.07	009 ARN 62.11 112.18 0.00	009 MHR 67.82 115.68 0.00	009 PWR 74.66 114.88 0.00	009 JCL 83.19 115.53 0.00	010 FGR 6.68 1 1.52 0.00	010 BCR 18.45 16 4.12 0.06	010 S02 20.51 2 3.90 0.04	010 S16 22.85 2 4.80 0.00	010 PDR 24.15 13 5.20 0.08	010 STV 26.72 15 5.54 0.09	010 S03 30.30 2 5.95 0.00	010 ALM 31.87 12 6.03 0.08	010 EUC 32.82 2 6.67 0.14	010 LTN 34.04 14 6.78 0.10	010 SFT 39.67 1 7.87 0.00	010 CBO 44.05 1 8.47 0.00	010 FMR 44.24 2 8.80 0.04	010 DIL 53.10 2 9.80 0.00	010 CHR 53.71 3 9.90 0.03	010 ANZ 55.29 1 6.82 0.00	010 SJG 60.56 311.02 0.00	010 CAN 61.87 1 9.02 0.00	010 SRS 72.25 1 8.57 0.00	010 PNC 72.38 1 8.17 0.00						

PHL S-5	51.09	9.82	
PHL S-4	51.55	9.86	
PHL S10	51.59	10.59	R
PHL LRV	52.11	10.74	
PHL S-1	52.86	10.04	
PHL S03	53.84	10.34	RE
PHL H-2	56.75	11.07	
PHL H-1	56.44	10.79	
PHL SP5J	56.44	10.79	RE
PHL COE	57.22	11.74	E
PHL ALM	59.57	11.24	
PHL S02	61.91	11.78	R
PHL ARN	61.08	11.69	
PHL SVC	64.85	12.59	
PHL S16	65.83	12.24	
PHL MHR	70.73	13.69	
PHL CAL	81.37	15.29	
PHL JDL	83.44	15.44	
PHL STV	87.60	16.24	
PHL STJ	88.69	16.84	
PHL LTW	97.91	16.74	
PHL SFT	99.50	17.64	
USGS SAN JOSE SHOT			
SHOT SITE	DELTA	T	SOLN
SP5J H-3	0.27	0.14	
SP5J H-2	0.35	0.12	
SP5J H-1	0.47	0.14	
SP5J S-1	4.62	1.19	
SP5J S-2	5.12	1.28	
SP5J S-3	5.41	1.36	
SP5J S-4	5.81	1.37	
SP5J S-5	6.30	1.57	
SP5J S-6	6.83	1.69	
SP5J ALM	9.01	2.09	
SP5J SVC	9.75	2.54	
SP5J COE	10.10	2.14	
SP5J CBD	11.38	2.54	
SP5J S11	11.75	2.71	
SP5J AND	12.55	2.89	
SP5J J-1	13.00	2.97	
SP5J J-2	13.43	3.04	
SP5J J-4	14.23	3.20	
SP5J J-5	14.67	3.26	
SP5J J-6	15.15	3.35	E
SP5J S03	15.21	3.36	RE
SP5J EUC	16.95	3.49	
SP5J MHR	17.92	4.44	RE
SP5J S16	18.04	3.74	RE
SP5J S04	19.04	4.14	RE
SP5J S12	19.34	4.04	RE
SP5J S10	20.21	4.64	R
SP5J K-2	20.79	4.39	E
SP5J S13	21.77	4.64	RE
SP5J S02	22.31	4.66	
SP5J S14	24.06	4.94	RE
SP5J BCR	24.12	5.09	R
SP5J S09	24.22	5.62	R
SP5J HCC	24.26	5.34	RE
SP5J ARN	26.13	5.64	RE
SP5J S18	26.80	5.54	RE
SP5J PMR	27.75	5.94	RE
SP5J CAL	28.33	6.24	RE
SP5J CHR	30.71	6.09	RE
SP5J CBC	30.86	6.64	R
SP5J CAN	31.07	6.64	RE
SP5J S08	32.34	6.78	RE
SP5J STJ	33.19	7.14	
SP5J CRC	33.38	6.84	
SP5J S07	33.45	6.64	
SP5J STV	33.82	6.69	
SP5J PEM	33.84	6.99	RE
SP5J Q04	34.38	7.13	RE
SP5J EGR	35.71	6.94	R
SP5J ANZ	37.84	7.64	RE
SP5J OCR	38.32	7.54	RE
SP5J POR	41.01	8.14	R
SP5J DIL	41.51	8.09	R
SP5J Q-3	43.13	8.56	
SP5J LTM	43.14	8.59	RE
SP5J SFT	43.57	8.64	RE
SP5J Q-4	43.60	8.66	
SP5J Q-5	44.08	8.84	
SP5J Q-6	44.40	8.91	
SP5J MHR	45.31	9.14	E
SP5J RAV	45.91	8.70	
SP5J SJG	47.29	9.04	R
SP5J CYH	49.86	9.19	RE
SP5J PAL	51.18	9.99	RE
SP5J WDS	51.69	9.89	
SP5J FDR	52.66	11.04	
SP5J S15	53.01	9.99	RE
SP5J P-6	53.89	10.57	
SP5J P-5	54.24	10.57	
SP5J P-4	54.65	10.59	
SP5J P-3	55.00	0.66	
SP5J P-1	55.74	10.73	
SP5J T-1	55.92	10.72	E
SP5J T-2	56.44	10.80	
SP5J T-3	56.70	10.79	
SP5J SRS	62.52	11.34	R
SP5J QSR	63.29	11.69	
SP5J CHR	64.63	12.79	
SP5J PNC	71.40	12.79	
SP5J SAL	72.30	12.89	
SP5J STC	78.21	15.74	
SP5J ANG	94.57	16.94	
SP5J SHG	97.99	16.94	
SP5J JDL	134.43	22.54	
BIG BASIN SHOT (STEWART,1968)			
SHOT SITE	DELTA	T	SOLN
BBN2 POR	4.43	1.25	
BBN2 KIN1	11.09	2.88	
BBN2 STV	11.36	3.07	
BBN2 KIN2	11.38	2.86	
BBN2 KIN3	11.59	2.94	
BBN2 BMT	11.63	3.25	
BBN2 LHD	12.65	3.34	RM
BBN2 LTW	14.48	3.74	RM
BBN2 STJ	17.07	4.14	
BBN2 LOVE	18.64	3.57	
BBN2 STH3	20.43	4.92	
BBN2 SFT	20.64	4.92	
BBN2 STH2	20.87	4.96	
BBN2 STH1	21.68	5.12	
BBN2 WDS	21.79	5.01	RM
BBN2 WAST	22.35	4.81	W
BBN2 TREE	37.79	7.65	W
BBN2 CYH	38.42	7.68	
BBN2 ELG3	38.60	7.62	
BBN2 ELG2	39.24	7.74	
BBN2 ELG1	39.89	7.81	
BBN2 LIND	48.95	10.00	W
BBN2 RAB8	59.65	11.80	RM
SAN JUAN SHOT (STEWART,1968)			
SHOT SITE	DELTA	T	SOLN
SJN 8K1	2.86	0.68	
SJN SJG	3.39	0.77	
SJN 6L6	3.63	0.84	
SJN 8K6	5.05	2.21	
SJN 6L1	5.51	1.29	
SJN 9J1	7.72	1.60	
SJN 9J6	7.95	1.65	
SJN 5P6	10.98	2.39	
SJN 10S1	12.27	2.64	MS
SJN 10S6	12.47	2.51	
SJN 5P1	13.23	2.80	WN
SJN 11T1	14.06	2.87	WN
SJN 11T6	16.38	4.28	
SJN OCR	17.51	4.32	
SJN 12R1	17.54	3.51	MS
SJN RAB8	17.68	3.68	RWN
SJN 12R6	19.93	3.84	
SJN 13Q1	21.32	4.03	MS
SJN TYNA	22.49	4.52	WN
SJN 13Q6	23.17	4.38	
SJN PHR	23.24	4.71	RWN
SJN 14L1	25.47	4.77	
SJN 14L6	27.60	5.04	MS
SJN 15S1	28.64	5.29	MS
SJN LIND	28.68	5.75	WN
SJN 15S6	30.43	5.59	
SJN 16P1	30.90	5.66	MS
SJN 4Q6	32.85	6.48	WN
SJN 16P6	33.06	6.02	
SJN 17K1	34.18	6.19	MS
SJN 4Q1	34.93	6.95	
SJN 18J1	35.85	6.49	
SJN 18J6	37.79	6.80	MS
SJN TREE	39.57	7.53	WN
SJN 19T1	40.72	7.25	WN
SJN 19T4	42.00	7.47	
SJN 20S1	42.53	7.55	MS
SJN 3R1	44.55	8.17	
SJN 20S6	44.57	7.86	
SJN 22Q1	47.88	8.39	MS
SJN 23P1	49.95	8.75	MS
SJN REDM	51.83	9.54	
SJN 23P6	51.94	9.02	
SJN 24S1	53.86	9.31	MS
SJN WAST	54.88	9.96	WN
SJN 24S6	55.78	9.60	
SJN 25K1	55.93	9.64	MS
SJN 25K6	57.77	9.91	
SJN 26J1	59.11	10.29	MS
SJN 26J6	60.90	10.60	
SJN 27T1	61.98	10.61	MS
SJN 27T6	63.83	10.89	
SJN 28R1	65.15	11.18	MS
SJN 28R6	67.32	11.47	
SJN 29Q6	68.12	11.68	MS
SJN 29Q6	69.36	11.78	
SJN 1T6	75.54	13.21	
SJN 1T1	77.02	13.33	
GONZALES SHOT (STEWART,1968)			
SHOT SITE	DELTA	T	SOLN
GNZ 18J6	0.99	0.28	
GNZ 18J1	1.14	0.27	
GNZ 17K6	2.48	0.54	
GNZ 19T1	4.08	0.86	
GNZ 16P6	4.40	0.90	
GNZ 17K1	4.22	0.86	
GNZ 20S1	5.86	1.21	
GNZ 19T4	5.32	1.11	
GNZ 16P1	6.49	1.30	
GNZ 15S6	7.29	1.39	
GNZ 15S1	8.85	1.75	
GNZ 20S6	8.09	1.63	
GNZ 14L6	9.39	1.89	
GNZ 22Q1	11.03	2.21	
GNZ 14L1	11.47	2.22	
GNZ 23P1	13.20	2.63	MS
GNZ 13Q6	14.09	2.81	
GNZ 23P6	15.25	2.97	
GNZ 13Q1	16.11	3.17	MS
GNZ 24S1	17.24	3.25	MS
GNZ 12R6	18.10	3.42	
GNZ 24S6	19.50	3.58	
GNZ 25K1	19.08	3.62	MS
GNZ 12R1	20.03	3.75	MS
GNZ 11T6	20.79	3.96	
GNZ 25K6	20.91	3.91	
GNZ 26J1	22.26	4.21	MS
GNZ 11T1	23.12	4.36	MS
GNZ 26J6	24.08	4.55	
GNZ 10S6	24.40	4.78	
GNZ 10S1	24.71	4.62	MS
GNZ 27T1	25.13	4.63	MS
GNZ 27T6	26.78	4.93	
GNZ 28R1	28.30	5.16	MS
GNZ 9J6	29.26	5.32	
GNZ 9J1	29.16	5.32	
GNZ 28R6	30.44	5.50	
GNZ 29Q1	31.29	5.74	MS
GNZ 8K6	31.87	5.84	MS
GNZ 29Q6	32.48	5.83	
GNZ 30P1	33.23	6.00	
GNZ 8K1	34.13	6.29	
GNZ 30P6	35.12	6.34	
GNZ 31H1	36.95	6.58	MS
GNZ 7H1	38.03	6.80	RWS
GNZ 31H6	38.15	6.78	
GNZ 5J6	39.32	7.06	RWS
GNZ 6L6	40.34	7.25	
GNZ R1S1	42.73	7.83	MS
GNZ R1S2	42.22	7.57	
GNZ R1S3	43.37	7.91	
GNZ 5P6	47.80	8.63	
GNZ 5P1	50.08	8.99	MS
GNZ NAT2	50.98	9.26	
GNZ NAT1	51.55	9.43	
GNZ NAT3	52.28	9.57	
GNZ RAB8	54.54	10.15	RM
GNZ TYNA	59.32	10.87	W
GNZ MIND	66.33	11.84	MS
GNZ 4Q6	69.71	12.48	W
GNZ PANC	70.08	12.33	
GNZ SARG	76.05	13.29	
GNZ IND2	82.96	14.59	
HERNANDEZ SHOT (STEWART,1968)			
SHOT SITE	DELTA	T	SOLN
HRN 30P6	2.33	0.62	
HRN REYN	2.59	0.81	
HRN 30P1	4.52	0.94	
HRN R1S2	5.01	1.25	
HRN R1S1	5.46	1.40	
HRN 29Q6	5.67	1.20	
HRN R1S3	6.07	1.51	
HRN 29Q1	6.21	1.35	
HRN 28R6	7.76	1.58	
HRN 28R1	9.61	1.94	
HRN 27T6	11.23	2.25	
HRN 27T1	12.52	2.49	MS
HRN 26J6	13.39	2.72	
HRN NAT2	13.71	3.02	
HRN NAT1	14.22	3.16	W
HRN NAT3	14.96	3.27	
HRN 26J1	15.32	3.00	
HRN 25K6	16.82	3.15	
HRN BLAC	20.14	3.77	MS
HRN 24S6	20.96	3.80	
HRN 32L1	21.07	4.24	
HRN 24S1	22.26	4.02	MS
HRN 32L6	22.76	4.50	
HRN 23P6	23.15	4.24	
HRN BR0W	24.51	4.71	MS
HRN 23P1	24.87	4.49	MS
HRN 22Q1	26.60	4.82	MS
HRN WIND	29.20	5.70	MS
HRN 20S6	30.30	5.42	
HRN 20S1	32.04	5.67	MS
HRN 19T4	32.53	5.83	
HRN PANC	32.95	6.11	MS
HRN 19T1	33.78	6.02	MS
HRN 18J6	36.43	6.42	MS
HRN 18J1	38.45	6.77	
HRN 17K6	39.49	7.08	
HRN 33L1	39.99	7.49	
HRN 17K1	40.01	7.04	MS
HRN 16P6	41.08	7.27	
HRN 16P1	43.26	7.62	MS
HRN 15S6	43.77	7.68	
HRN IND1	45.38	8.26	MS
HRN 15S1	45.56	8.03	MS
HRN IND2	45.93	8.31	

RANCHITO SHOT (STEWART,1968)

SHOT SITE	DELTA	T	SOLN
RAN IND3	11.97	3.12	
RAN IND2	12.68	3.25	
RAN IND1	13.26	3.36	WS
RAN SARG	19.69	4.55	
RAN PANC	25.65	5.52	WS
RAN WIND	29.40	6.29	WS
RAN BROW	34.10	7.21	WS
RAN BLAC	38.51	7.69	WS
RAN BLAR	39.66	7.98	
RAN RIS3	52.53	9.90	
RAN RIS1	53.14	10.00	WS
RAN RIS2	53.61	10.12	
RAN REYN	56.08	10.56	

BENICIA SHOT (STEWART,1968)

SHOT SITE	DELTA	T	SOLN
BEN AZEV	7.99	2.04	
BEN UTAH	8.06	2.35	
BEN MILA	11.64	3.40	
BEN NOGA	13.75	3.91	
BEN CANA	18.84	5.02	
BEN PARA	24.18	5.80	
BEN DIAB	31.62	6.61	
BEN MT01	33.20	7.73	E
BEN MT02	34.04	7.77	
BEN AT03	34.72	7.49	
BEN HAWK	36.63	8.23	E
BEN TASS	41.30	9.22	E
BEN MUR1	50.06	10.91	E
BEN MUR2	50.76	10.91	
BEN MUR3	51.56	11.17	
BEN MEN1	66.95	13.73	
BEN MEN2	67.72	13.79	
BEN MEN3	68.50	13.71	
BEN 10J6	85.27	15.97	
BEN 10J1	87.27	16.24	
BEN 11K1	88.01	16.28	
BEN 11K6	90.27	16.58	
BEN 12R1	90.75	16.69	
BEN 13H1	94.11	17.30	
BEN 13H6	96.32	17.50	
BEN 14Q1	97.00	17.59	
BEN 14Q6	99.19	17.87	
BEN 15S1	100.91	18.62	
BEN 15S6	102.93	18.82	

CEDAR MTN SHOT (STEWART,1968)

SHOT SITE	DELTA	T	SOLN
CED 771	0.85	0.31	
CED 776	0.96	0.28	
CED 8P1	2.03	0.62	
CED 8P6	4.25	1.30	
CED 651	4.83	1.26	
CED 656	2.94	0.87	
CED 9R1	5.08	1.46	
CED 9R6	7.37	1.95	
CED 10J1	8.70	2.16	
CED MEN3	9.16	2.20	
CED MEN2	10.06	2.46	
CED MEN1	10.82	2.69	
CED 10J6	10.85	2.62	
CED 11K1	11.59	2.88	
CED 501	12.53	3.06	
CED 11K6	13.99	3.24	
CED 12R1	14.63	3.42	
CED 13H1	18.07	4.46	
CED 13H6	20.23	4.07	
CED MUR3	25.43	6.36	
CED MUR2	26.21	6.51	
CED MUR1	26.85	6.63	E
CED 15S6	27.61	5.88	
CED 16T1	28.46	6.06	
CED 4J1	31.35	7.47	
CED 4J6	29.29	7.17	
CED 19J1	39.62	7.95	
CED TASS	35.56	8.40	E
CED 19J6	39.62	7.95	
CED HAWK	40.47	9.25	E
CED 20K6	41.82	8.26	E
CED MT03	42.09	9.85	
CED MT02	42.77	9.73	
CED 21L1	42.92	8.47	E
CED MT01	43.64	9.53	E
CED 21L6	45.01	8.85	
CED 22P6	47.00	9.16	
CED 23Q1	47.58	9.22	E
CED 22P1	47.61	9.31	E
CED 23Q6	49.53	9.58	E
CED 24R6	50.11	9.66	
CED 24R6	50.64	9.79	
CED 26T6	55.33	10.60	E
CED 27S6	58.78	11.19	
CED WRIG	79.23	14.75	
CED WILD	84.77	15.96	
CED WILD	84.85	16.03	
CED M011	94.21	17.89	

MT STAKES SHOT (STEWART,1968)

SHOT SITE	DELTA	T	SOLN
MTS 17P6	0.70	0.28	
MTS 17P1	1.22	0.37	
MTS 18L1	1.26	0.41	

MTS 16T6	2.14	0.58	
MTS 16L6	3.36	0.70	
MTS 16T1	4.43	1.18	
MTS 15S6	5.28	1.34	
MTS 19J1	5.31	1.35	
MTS 19J6	6.73	1.69	
MTS 20K1	6.98	1.73	
MTS 20K6	8.96	2.14	
MTS 14Q6	9.48	2.31	
MTS 21L1	10.04	2.35	
MTS 14Q1	11.89	2.69	
MTS 21L6	12.13	2.79	
MTS 13H6	12.85	3.30	
MTS 22P6	14.42	3.23	
MTS 22P1	14.78	3.34	
MTS 13H1	14.89	2.87	
MTS 23Q1	15.33	3.34	
MTS 12R6	16.32	3.62	
MTS 23Q6	17.37	3.74	
MTS 12R1	18.31	4.01	
MTS 24R1	18.36	3.88	
MTS 11K6	19.00	4.10	
MTS 24R6	19.39	4.10	
MTS 25S1	19.80	4.16	
MTS 25S6	21.65	4.56	
MTS 26T6	24.37	5.02	E
MTS 9R6	25.69	5.28	
MTS 27S1	26.53	5.43	
MTS 27S6	27.62	5.59	
MTS 9R1	27.88	5.80	
MTS 28L1	29.79	6.00	
MTS 8P1	30.88	6.39	
MTS 28L6	32.16	6.35	
MTS 7T1	33.74	6.92	E
MTS 29J1	33.79	6.62	
MTS 656	35.65	7.11	
MTS 651	36.94	7.27	E
MTS 30H6	38.45	7.45	
MTS MEN2	40.54	8.16	
MTS MEN1	41.27	8.22	
MTS SANL	42.96	8.20	E
MTS MUS1	53.43	10.06	E
MTS HERR	56.52	10.68	E
MTS MUS3	54.15	10.18	
MTS MUR2	57.42	11.86	
MTS MUR1	58.18	11.96	
MTS 33P1	63.46	12.47	
MTS ENG3	68.99	12.78	
MTS MISE	68.80	12.87	
MTS ENGL	69.01	12.70	
MTS MINE	77.16	14.42	

PACHEGO SHOT (STEWART,1968)

SHOT SITE	DELTA	T	SOLN
PCH 32K1	2.09	0.56	
PCH 30H1	2.84	0.48	
PCH SANL	3.38	0.85	
PCH 32K6	4.07	0.98	
PCH 29J6	4.30	1.02	
PCH 29J1	6.04	1.37	
PCH 28L6	7.70	1.74	
PCH WRIG	8.46	2.97	
PCH 28L1	9.99	2.19	
PCH 27S6	12.07	2.56	
PCH 27S1	13.36	2.81	
PCH WILD	14.04	2.93	
PCH MUS2	14.44	2.69	
PCH MUS1	15.15	3.28	E
PCH 26T6	15.48	3.28	E
PCH 25S6	18.29	3.82	
PCH 24R6	20.34	4.17	
PCH 24R1	21.23	4.36	E
PCH 23Q6	22.31	4.52	
PCH 23Q1	24.36	4.92	E
PCH 22P6	25.57	5.19	
PCH 22P1	26.12	5.36	E
PCH 21L6	28.97	5.79	
PCH WISE	29.48	5.83	E
PCH 19J1	35.39	7.01	
PCH 21L1	30.65	6.11	E
PCH 20K6	31.38	6.27	E
PCH QRT1	33.65	6.78	E
PCH 19J6	33.77	6.71	
PCH 18L6	37.05	7.23	
PCH 18L1	38.53	7.44	
PCH VASQ	41.55	8.06	
PCH 35R6	51.93	10.08	
PCH 35R1	49.86	9.61	E

PANOCHE SHOT (STEWART,1968)

SHOT SITE	DELTA	T	SOLN
PAN VASQ	9.96	2.17	
PAN MINE	13.48	2.87	
PAN CER2	14.56	3.09	
PAN GER1	15.30	3.33	
PAN QRT1	17.58	3.59	E
PAN ENG3	21.72	4.40	
PAN WISE	21.74	4.37	E
PAN ENGL	21.87	4.44	
PAN HERR	34.07	6.35	E
PAN MUS3	36.34	7.15	E
PAN MUS1	37.05	7.24	
PAN WILD	37.17	7.15	
PAN MUS2	37.62	7.36	
PAN WRIG	42.80	8.19	
PAN SANL	47.91	9.07	E

PAN 26T6	66.69	12.48
PAN 25S6	69.49	12.99
PAN 25S1	71.39	13.25
PAN 24R6	71.48	13.40
PAN 23Q1	75.10	13.94
PAN 22P6	76.07	14.04
PAN 22P1	76.13	14.06
PAN 21L1	80.92	14.88
PAN 19J6	84.21	15.39
PAN 17P3	90.90	16.78
PAN 10J6	111.24	20.82
PAN 9R6	114.63	20.96
PAN 9R1	116.94	21.24

BEAR VALLEY SHOT (EATON,UNPUBLISHED DATA)

SHOT SITE	DELTA	T	SOLN
BVSP A18V	1.19	0.41	
BVSP J18V	8.46	1.76	
BVSP J06V	9.78	2.05	
BVSP HP2	9.79	1.99	
BVSP L18V	11.31	3.17	
BVSP HP8	11.84	3.05	
BVSP HP5	12.77	3.34	
BVSP HP7	12.98	2.63	
BVSP HP12	14.07	3.80	
BVSP HP9	14.44	2.78	WS
BVSP HP3	17.53	3.48	
BVSP HP6	17.54	3.38	
BVSP F18V	17.71	4.48	
BVSP T68V	18.44	4.35	
BVSP HP4	19.59	4.70	
BVSP HP10	22.44	5.17	
BVSP P18V	25.71	5.20	
BVSP P68V	28.26	5.40	
BVSP HP11	29.67	6.18	
BVSP K18V	31.75	6.63	
BVSP K68V	32.78	6.86	
BVSP R18V	35.59	7.58	
BVSP R68V	35.65	7.72	
BVSP HP13	37.02	6.99	
BVSP HP14	38.05	6.97	RMS
BVSP HP15	39.22	7.13	
BVSP S18V	41.04	7.65	
BVSP S JG	41.49	7.42	RMS
BVSP S68V	41.93	7.55	
BVSP Q68V	44.16	9.35	
BVSP HP17	45.57	9.08	
BVSP Q18V	45.59	9.55	
BVSP ANZ	49.10	8.77	RM
BVSP HP16	52.84	9.25	
BVSP H68V	53.80	9.55	
BVSP PMR	61.04	11.47	
BVSP HP18	61.83	11.67	
BVSP STV	113.82	19.47	
BVSP POR	118.14	20.12	

PESCADERO SHOT (EATON,UNPUBLISHED DATA)

SHOT SITE	DELTA	T	SOLN
PESP ANZ	3.61	1.45	
PESP OGR	7.61	2.55	
PESP PMR	9.80	2.80	
PESP S JG	13.30	3.47	
PESP HP13	14.99	4.28	
PESP Q1PE	15.34	3.74	
PESP HP18	20.33	4.72	
PESP HP17	22.32	5.32	
PESP HP3	34.59	7.18	
PESP K1PE	34.95	7.40	
PESP HP4	36.42	8.18	
PESP L1PE	36.60	7.80	
PESP HP6	39.36	7.62	
PESP HP14	39.52	7.81	
PESP HP2	42.34	8.40	
PESP Q1PE	44.20	9.02	
PESP S1PE	45.43	8.85	
PESP HP10	48.89	10.30	
PESP HP7	49.15	9.32	
PESP HP5	49.91	10.20	
PESP HP1	51.00	9.67	
PESP HP16	55.72	10.45	
PESP H1PE	56.63	10.68	
PESP HP15	58.34	10.80	
PESP HP12	61.51	12.58	
PESP HP8	63.58	12.22	
PESP STJ	63.83	15.80	
PESP STV	62.07	11.45	
PESP HP9	62.79	11.46	
PESP POR	66.96	12.50	
PESP BMT	67.14	12.60	
PESP LTH	72.61	13.50	
PESP SFT	74.58	13.70	
PESP LHO	76.25	14.00	
PESP HP11	81.58	15.67	
PESP MDS	81.83	15.00	
PESP CYH	83.31	15.00	

NATIVIDAD QUARRY (TURCOTTE,1964)

SHOT SITE	DELTA	T	SOLN
Q031 T2Z	9.52	1.90	
Q031 T2Y	13.75	3.12	
Q031 TAC	16.67	4.90	
Q031 VIT	18.30	3.60	
Q031 TZX	22.49	5.20	
Q031 TAC	35.72	7.00	
Q031 SCC	45.64	8.50	

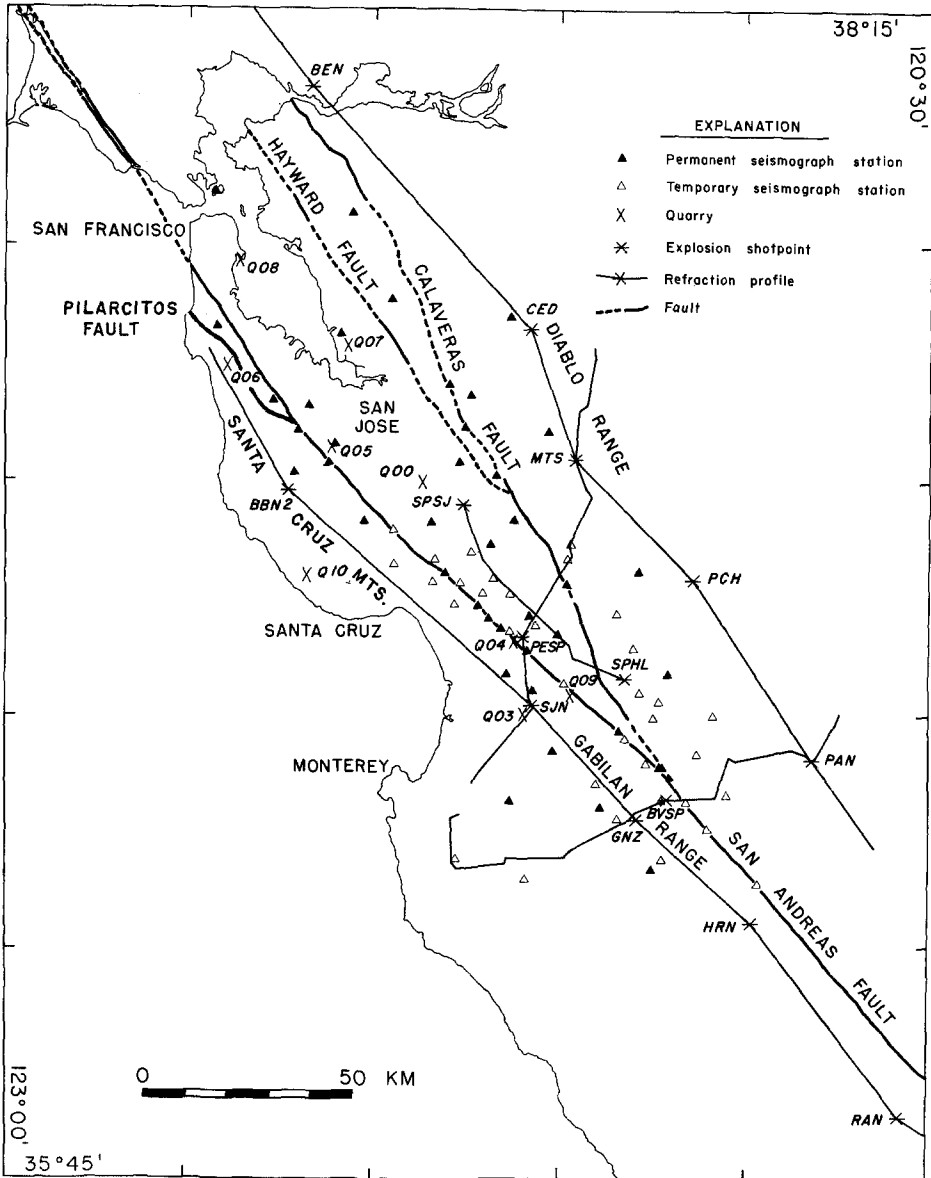


FIG. 1. San Francisco Bay area showing quarries, shots, permanent and temporary stations, lines of refraction profiles, major faults and ranges.

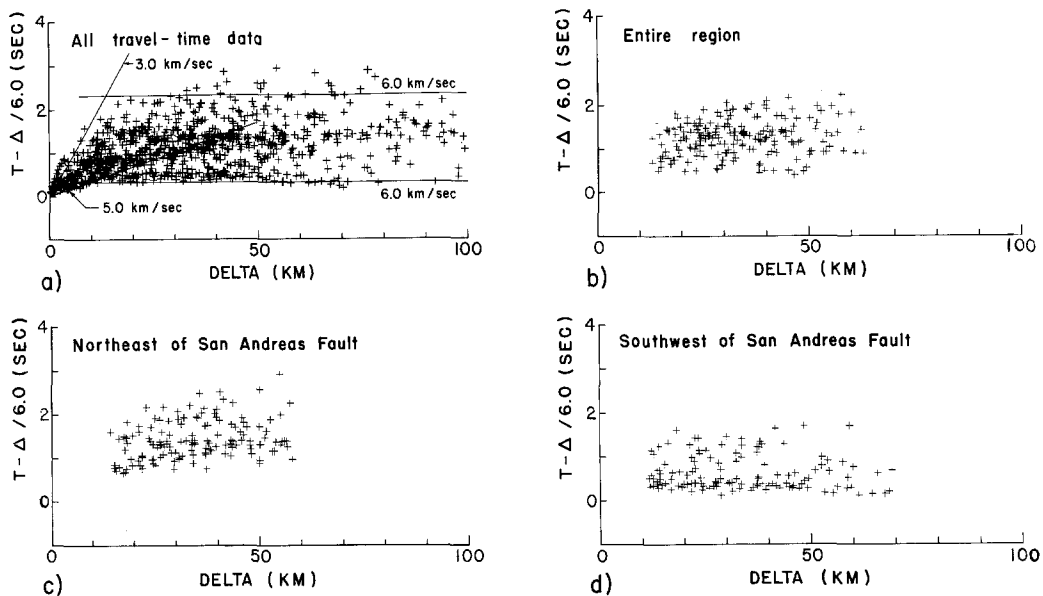


FIG. 2. Travel-time data. (a) All available data, (b) data used for time-term solutions sampling the entire region, (c) the region northeast of the San Andreas Fault, and (d) the region southwest of the San Andreas Fault.

a station, even though there is no statistical basis for assessing its reliability. If two neighboring sites are thought to have a similar geological setting (i.e., same near-surface velocity and depth to basement), they can be assigned the same time term, thus decreasing the number of degrees of freedom. A low mean residual of such a time term may be taken as evidence verifying the assumption. The time-term method also requires that at least one, and preferably several, of the source sites be used as a recording site. This was accomplished by assuming site equivalence (Table 3) between the uphole seismometer and the shot point and, in a few cases, between a quarry and a nearby station.

As the distance at which P_g first emerges as a first arrival is particularly sensitive to the structure in the vicinity of the source, travel-time curves were plotted for all shots and quarry blasts. P_g emerges as a first arrival at distances ranging from about 12 km for shots in the Gabilan Range, where granite is exposed at the surface, to about 25 km in the northern Diablo Range, where the P_g refractor is covered by at least 4 km of Cretaceous and Cenozoic sedimentary rocks.

The distance at which P_g is first preceded by refracted waves with higher velocities is much harder to identify because the change in velocity is subtler and the quality of the data, particularly southwest of the fault, begins to deteriorate at these distances. Travel-time curves were examined and data recorded at distances less than 58 km for the northeast side and 70 km for the southwest side were included. The cutoff on the northeast side is determined by the emergence of arrivals with a velocity near 6.8 km/sec. The cutoff distance for the southwest side is particularly arbitrary because of the high attenuation of arrivals at these distances (Stewart, 1968) and because any change of velocity with depth is likely to be continuous and gradual. Fortunately, because the changes in the travel-time curve at large distances due to a slightly higher velocity at depth are subtle, the time-term method is not particularly sensitive to small errors in identification of phases, and large errors are normally detected where time terms have abnormally high mean residuals.

TABLE 3
ASSUMED SITE EQUIVALENCES

Sites	Distances between Sites (km)	Solutions in Which Equivalence was Assumed*
CED = 7T1	0.85	E
GNZ = 18J6	0.99	WS
HRN = 31H1	0.90	WS
HP9 = 22Q1	1.04	WS
HP14 = PNC	0.11	RWS
IND1 = IND2	0.90	WS
MNR = 6S1	0.63	E
Q03 = SJG	4.08	N
Q04 = S08	2.31	WS
Q05 = PEM	0.66	RE
RAN = 34J1	1.15	WS
SJN = 7H1	1.20	RWS
SPHL = T-1	0.98	RE
SPSJ = H-1	0.47	RE

* Key: R, entire region; E, NE of San Andreas Fault; W, SW of San Andreas Fault; S, S of San Juan Bautista; and N, N of San Juan Bautista.

All data that met the foregoing criteria for the time-term method were included in the time-term analysis. Three sets of data (Table 2) on which analyses were performed are plotted in Figure 2 (b, c, and d). The first set was a sampling of data from the entire region, resulting in an "average" model. The two remaining sets of data (Figure 2, c and d) are travel times for the northeast and southwest sides of the San Andreas Fault.

No travel time assigned to one side of the fault had more than a small fraction of its travel path on the other side of the fault. The clear difference between the travel-time curves for the two data sets suggests, as expected, that this separation is justified. Data from the southwest side indicate a velocity of very nearly 6.0 km/sec; data from the northeast show a slightly lower velocity. Both data sets are scattered but in neither set is the scatter as large as for the total set.

Residuals as a function of distance for solutions from these three data sets are shown in Figure 3(a, b and c). The slightly lower standard deviations for the subdivided data sets relative to the solution for the entire data set are another indication that data taken separately for each side are more consistent internally than data from the total area. A further subdivision of the data from the southwest is discussed in a separate section.

INTERPRETATION OF TIME TERMS

Time terms calculated for the three data sets corresponding to the entire region and the regions northeast and southwest of the San Andreas Fault are given in Tables 4, 5 and 6, for stations or sources northeast, southwest, or adjacent to the San Andreas Fault, respectively. Time terms calculated for stations using data for the whole region are generally within 0.1 sec of the time terms calculated for the data sets northeast and southwest of the San Andreas Fault. This suggests that the time terms are not influenced

greatly by the slight differences in refractor velocity obtained in the solutions, nor are they influenced greatly by the particular subset of the data. Time terms at several stations, many of which are adjacent to the San Andreas Fault, showed a strong azimuthal variation. This was expected because the discontinuous geological structure across the fault violates the assumptions of low basement relief and small lateral change in near-surface velocity.

The calculated time terms for stations and sources northeast of the San Andreas Fault using data for the entire region and using data from northeast side alone are given in Table 4. Because the difference in refractor velocity between the two solutions is quite small, the differences in the time terms, as might be expected, are also quite small, averaging 0.04 sec. The number of data and mean residual for each time term (also shown in Table 4) demonstrate the quality and consistency of the data.

From time terms for stations and sources on the southwest side of the San Andreas Fault shown in Table 5, it is clear that the difference between the sets of time terms calculated using data from the entire region and those from the southwest side alone, which average 0.07 sec compared with 0.04 sec for the northeast side, reflects the larger difference in the refractor velocity obtained in the solution. That the average differences between the time terms calculated from the respective data sets are of the order of the mean residuals for the individual time terms indicates that these residuals are barely significant.

Because of the discontinuous geological structure across the San Andreas Fault, time terms for sites adjacent to the fault were expected to vary with the direction of the approaching ray. Stations adjacent to the fault were assigned two time terms in the average model calculation, one for rays approaching from the northeast, and another for rays approaching from the southwest (Table 6). For many of these stations, the two time terms for the different directions of approach differ significantly. In almost all cases, however, the time term calculated for one direction of approach in the average model calculation is within a few hundredths of a second of the time term calculated in the solution using data from that side of the fault only (Table 6). The agreement of the time terms calculated from two different assumptions about the homogeneity of the refractor velocity suggests that inhomogeneity in refractor velocity plays a less important role in the variation of time term with the direction of approach than basement relief and inhomogeneity of near-surface velocity. A striking example of this variation with direction of approach is Q09, which is located in the fault zone between the granitic Gabilan Range and the Tertiary sedimentary deposits of the Hollister Trough. Time terms for the average data set for the east and west are 1.06 and 0.45 sec, respectively, and the corresponding time terms for the two sides solved individually are 1.18 and 0.41 sec. The mean residual for all these time terms is 0.11 sec. The variation of the time term at a given site with the direction of the approaching ray can be substantial.

A few stations at some distance from the fault zone demonstrate substantially different time terms for different subdivisions of the data set. These differences may be attributed to a variation with direction of approach due to local geological structure or refractor velocity.

Computer-size limitations made it inconvenient to obtain a solution for the whole data set at one time. However, the excellent agreement between those time terms included in both the average solution and those for either the northeast or southwest subdivision suggests that such a solution is unnecessary. Since the combination of northeast and southwest subdivision solutions included the most data, these solutions were taken as representative and the corresponding time terms plotted on Figure 3.

Northeast of the San Andreas Fault. Geological interpretation of the *P_g* refractor on the northeast side of the San Andreas Fault is complicated by the total absence of direct

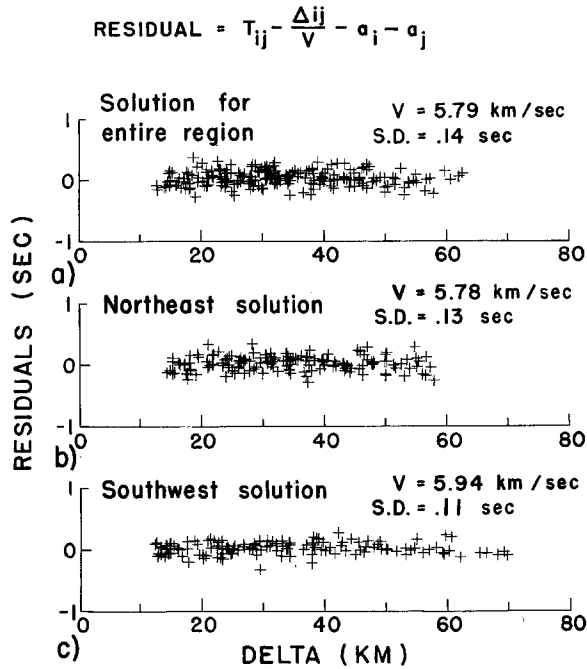


FIG. 3. Residuals plotted as a function of distance for the solutions corresponding to (a) the entire region, (b) the region northeast of the San Andreas Fault, and (c) the region southwest of the San Andreas Fault. The refractor velocity, v is that obtained from the time-term solution. S.D. is the standard deviation of the solution, as defined by Berry and West (1966).

TABLE 4
TIME TERMS FOR SITES NORTHEAST OF SAN ANDREAS FAULT

	Entire Region			NE of S.A. Fault		
	N	a_i	\bar{r}_i	N	a_i	\bar{r}_i
ALM	6	0.34	0.13	4	0.38	0.09
AND	5	0.45	0.09	4	0.45	0.13
ANG	2	0.43	0.00	2	0.42	0.01
ARN	3	0.65	0.07	3	0.66	0.05
BEN	—	—	—	4	0.65	0.10
BOL	3	0.85	0.04	3	0.86	0.05
CAL	5	0.75	0.12	5	0.76	0.14
CAN	4	0.62	0.11	4	0.59	0.09
CBC	2	0.80	0.13	—	—	—
CBO	4	0.30	0.06	4	0.38	0.09
CED	—	—	—	11	0.71	0.05
CHR	5	0.40	0.05	3	0.34	0.04
COE	6	1.04	0.07	6	1.14	0.11
CYH	3	0.34	0.10	3	0.34	0.12
HAWK	—	—	—	2	1.39	0.15
HCC	3	0.81	0.03	2	0.80	0.06
HERR	—	—	—	2	0.39	0.10
J-6	—	—	—	2	0.23	0.09
K-2	—	—	—	2	0.36	0.03
MHR	4	0.89	0.07	4	0.92	0.06
MNR	—	—	—	2	0.68	0.21
MTD1	—	—	—	2	1.30	0.04

Table 4—Continued

TABLE 4 (continued)

	Entire Region			NE of S.A. Fault		
	N	a_i	\bar{r}_i	N	a_i	\bar{r}_i
MTS		—		6	0.41	0.09
MURI		—		2	1.44	0.16
MUS1		—		3	0.35	0.11
OCR	4	0.58	0.12	3	0.46	0.10
ORT1		—		2	0.33	0.16
PAN		—		6	0.37	0.09
PAL	4	0.76	0.06	4	0.76	0.07
PCL	3	0.50	0.19	2	0.42	0.16
PCH		—		10	0.47	0.07
PVR	3	0.88	0.07	3	0.92	0.06
Q00	6	0.49	0.10	5	0.40	0.08
Q07*	13	-0.39	0.06	12	-0.41	0.06
Q08	8	0.12	0.08	8	0.13	0.09
QSR	3	0.63	0.10	2	0.58	0.21
SAL	3	0.55	0.02	2	0.56	0.02
SANL		—		2	0.38	0.02
SFT	4	0.75	0.04	3	0.74	0.05
SPHL	28	0.87	0.10	22	0.82	0.09
SPSJ	34	0.38	0.10	28	0.41	0.09
SVC	2	0.81	0.14	2	0.85	0.14
S03	6	0.25	0.12	3	0.30	0.06
S07	2	0.56	0.10		—	
S08	2	0.91	0.10	2	0.91	0.14
S11	3	0.11	0.05	2	0.10	0.02
S12	4	0.13	0.12	3	0.13	0.14
S13	4	0.46	0.12	3	0.49	0.04
S14	4	0.29	0.07	3	0.31	0.06
S15	4	0.72	0.18	3	0.62	0.21
S17	2	0.64	0.11		—	
S18	5	0.52	0.14	4	0.44	0.08
TASS		—		2	1.48	0.05
WISE		—		2	0.25	0.01
20K6		—		2	0.34	0.03
21L1		—		2	0.34	0.00
22P1		—		2	0.37	0.01
23Q1		—		2	0.26	0.02
24R1		—		2	0.25	0.03
26T6		—		3	0.28	0.10

Key: N, number of travel paths; a_i , time term; \bar{r}_i , mean residual = $(\sum_j |r_{ij}|)/N$.

*Time term includes uncertainty in origin time and therefore has no geological significance (see text).

TABLE 5
TIME TERMS FOR SITES SOUTHWEST OF THE SAN ANDREAS FAULT

Site	Entire Region			SW of S.A. Fault			N of San Juan Bautista			S of San Juan Bautista		
	N	a_i	\bar{r}_i	N	a_i	\bar{r}_i	N	a_i	\bar{r}_i	N	a_i	\bar{r}_i
BBN2	4	0.69	0.08	7	0.78	0.13	7	0.45	0.05			
BCR	3	0.60	0.04									
BLAC		—		2	0.43	0.16				2	0.43	0.19
BROW		—		2	0.56	0.09				2	0.56	0.11
BVSP	3	0.12	0.11	4	0.26	0.09				3	0.30	0.07
DIL	4	0.49	0.13	2	0.49	0.00						
GNZ	3	0.07	0.09	22	0.20	0.05				19	0.27	0.03
HRN		—		22	0.11	0.05				22	0.20	0.05
IND1		—		2	0.41	0.10				2	0.41	0.13
JHC	3	-0.11	0.09	3	0.09	0.08				3	0.26	0.06
LIND		—		2	0.88	0.11	2	0.84	0.01			
LHD	3	0.57	0.10	2	0.56	0.13	2	0.72	0.08			
NAT1		—		2	0.61	0.05				2	0.61	0.01
PANC		—		2	0.42	0.03				2	0.42	0.04
PNC	5	0.12	0.12	4	0.13	0.17				4	0.26	0.12
POR	5	0.81	0.08	2	0.79	0.02	2	0.82	0.02			
Q03	31	0.44	0.10	12	0.36	0.11	8	0.15	0.05	5	0.35	0.07
Q06*	5	-1.66	0.07	5	-1.54	0.06	5	-1.85	0.05			
Q10	14	0.28	0.08	9	0.37	0.10	9	0.11	0.03			
RABB	3	0.69	0.08	3	0.77	0.15	2	0.73	0.02			
RAN		—		7	0.82	0.08				7	0.89	0.09
RIS1		—		2	0.34	0.10				2	0.39	0.09
SHG	3	-0.19	0.10	2	0.00	0.06				2	0.21	0.01
SJG	6	0.30	0.16	4	0.27	0.09				3	0.28	0.02
SJN	3	0.02	0.09	27	0.15	0.08	8	-0.17	0.02	12	0.25	0.03
SRS	4	0.07	0.15	2	0.05	0.00				2	0.23	0.03
S02	4	0.19	0.14	2	0.19	0.12	2	0.12	0.02			
S09	4	0.96	0.09	2	1.03	0.12	2	0.92	0.17			
S10	5	0.82	0.13	3	1.04	0.17	2	0.73	0.08			
TREE		—		2	0.62	0.10	2	0.58	0.09			
TYNA		—		2	0.49	0.10						
WAST		—		2	0.42	0.15	2	0.39	0.00			
WIND		—		3	0.56	0.08				3	0.59	0.05
4Q6		—		2	0.68	0.12						
5P1		—		2	0.39	0.03						
8K6		—		2	0.22	0.06				2	0.27	0.02
10S1		—		2	0.34	0.08				2	0.30	0.05
11T1		—		3	0.29	0.04				3	0.29	0.02
12R1		—		3	0.28	0.08				3	0.28	0.08
13Q1		—		2	0.27	0.01				2	0.24	0.01
14L6		—		2	0.26	0.02				2	0.27	0.05
15S1		—		2	0.28	0.03				2	0.29	0.00
16P1		—		2	0.27	0.04				2	0.27	0.01
17K1		—		2	0.24	0.05				2	0.24	0.03
19T1		—		2	0.23	0.01				2	0.24	0.01
20S1		—		2	0.20	0.04				2	0.21	0.04
22Q1		—		3	0.17	0.05				3	0.17	0.05
23P1		—		3	0.20	0.01				3	0.19	0.02
24S1		—		3	0.12	0.02				3	0.12	0.02
25K1		—		2	0.14	0.07				2	0.15	0.04
26J1		—		3	0.26	0.05				3	0.25	0.01
27T1		—		3	0.17	0.10				3	0.17	0.06
28R1		—		2	0.13	0.07				2	0.17	0.04
29Q1		—		2	0.17	0.11				2	0.21	0.08

KEY: N, number of travel paths; a_i , time term; \bar{r}_i , mean residual = $(\sum_j |r_{ij}|)/N$.

*See footnote to Table 4.

TABLE 6
TIME TERMS FOR SITES ADJACENT TO THE SAN ANDREAS FAULT

Site	Entire Region						NE of S.A. Fault			SW of S.A. Fault			N of San Juan Bautista			S of San Juan Bautista		
	Arrivals from NE		Arrivals from SW		N	\bar{r}_i	N	a_i	\bar{r}_i	N	a_i	\bar{r}_i	N	a_i	\bar{r}_i	N	a_i	\bar{r}_i
	N	a_i	N	a_i														
ANZ	2	0.80	0.08	3	0.15	0.07	2	0.80	0.12	3	0.26	0.06	—	—	—	—	—	—
CNR	—	—	—	2	0.04	0.13	—	—	—	2	0.18	0.09	—	—	—	2	0.32	0.16
EUC	—	—	—	3	0.76	0.10	—	—	—	3	0.91	0.09	3	0.77	0.03	—	—	—
LTW	2	0.74	0.02	3	0.60	0.03	2	0.72	0.01	3	0.60	0.05	3	0.68	0.04	—	—	—
PMR	2	0.74	0.09	3	0.85	0.09	2	0.86	0.12	3	0.82	0.12	3	0.81	0.04	—	—	—
Q04	12	0.76	0.09	9	0.49	0.18	14	0.72	0.13	10	0.46	0.08	5	0.46	0.09	5	0.38	0.05
Q05	17	0.75	0.10	7	0.46	0.10	18	0.70	0.11	—	—	—	—	—	—	5	—	—
Q09	9	1.06	0.11	8	0.45	0.12	12	1.18	0.12	8	0.41	0.11	—	—	—	5	0.24	0.10
STC	—	—	—	2	—	—	2	1.00	0.19	—	—	—	—	—	—	—	—	—
STV	—	—	—	2	0.63	0.01	—	—	—	2	0.66	0.01	2	0.66	0.02	—	—	—
S04	—	—	—	—	—	—	2	0.62	0.19	2	1.09	0.13	2	0.95	0.10	—	—	—
S16	—	—	—	—	—	—	2	0.08	0.13	2	0.74	0.15	2	0.58	0.05	—	—	—
WDS	2	0.75	0.01	3	0.51	0.10	3	0.62	0.17	2	0.44	0.13	2	0.59	0.10	—	—	—

Key: N, number of travel paths; a_i , time term; \bar{r}_i , mean residual = $(\sum_j |r_{ij}|)/N$.

observations of a "crystalline" basement beneath the Franciscan Formation. No crystalline basement is exposed nor has any been penetrated by drilling. Inclusions in the ultramafic rocks that intrude the Franciscan suggest that it "was deposited directly upon basalt, peridotite or serpentine" (Bailey *et al.*, 1964). This hypothesis is supported by the similarity between the depositional environment of the Franciscan and that of the modern sea floor. The velocity profiles reported by Stewart (1968) for the Diablo Range are similar to those reported by Raitt (1963) and Shor *et al.* (1968) for the floor beneath the northeastern Pacific Ocean. While the velocities are not unique to a particular rock type, the velocities for oceanic crustal layers 2 and 3 are similar to the velocities obtained by Stewart (Table 7).

TABLE 7
COMPARISON OF THE VELOCITIES OF CRUSTAL ROCKS
UNDERLYING FRANCISCAN TERRAIN AND THE NORTH-
EASTERN PACIFIC OCEAN

Franciscan Terrain, Velocity* (km/sec)	Ave. NE Pacific, Velocity† (km/sec)	
5.5-5.70	Layer 2	5.65
6.86	Layer 3	6.75
8.18	Layer 4	8.24

* Stewart, 1968.

† Raitt, 1963.

East of the Calaveras Fault, rocks of the Franciscan Formation rise in a broad arch, the Diablo antiform (Bailey *et al.*, 1964). The axis of this structure trends northwest, roughly paralleling the fault zones. Time terms generally increase from about 0.3 sec in the south to about 1.5 sec in the north. This indicates the general dip of the *Pg* refractor to the northwest pointed out by Stewart (1968). Depths to the refractor calculated from the time terms, assuming the velocities above the refractor given by Stewart, are in substantial agreement with the refractor depths he reported for the region between the shot points CDM and PCH. This should be expected, as the data sets are substantially the same. Calculated depths to the refractor range from about 2.0 to 4.5 km. Stewart did not give an interpretation corresponding to the very large time terms, 1.3 to 1.5 sec, just south of Mount Diablo; apparently, the *Pg* refractor is either very deep in this region or is covered by a very low-velocity material. He recorded an arrival on Mount Diablo that was more than $\frac{1}{2}$ sec early relative to a well-determined *Pg* branch. It probably resulted from the relatively high-velocity ultramafic rocks which form the mountain. The time term calculated for the Benicia shot point (0.65 sec) in the extreme northern part of the area may indicate a reversal of the northward dip of the refractor, but it is inconclusive. Along the western margin of the Diablo antiform and between the Calaveras and Hayward Faults, time terms range from 0.5 to 1.1 sec. These larger time terms indicate a thicker sedimentary cover. Very large time terms are observed at stations just north of the point where the Hayward and Calaveras Faults branch, an area over a pronounced gravity-low (Robbins, 1971). The structural discontinuities implied by these faults might be expected to produce variations in time terms with the direction of the approaching ray. As no arrivals were observed from the east, it was not possible to demonstrate the existence of this effect. There is a high density of time terms in the vicinity of the Sargent Fault between San Jose and Hollister and they are remarkably

consistent with mapped geological structure. Time terms decrease from 0.4 to 0.1 sec from the north and east toward the Sargent Fault. This trend coincides with a thinning in the sedimentary cover, the exposure of rocks of the Franciscan Formation, and a change in the character of the exposed rocks in the Franciscan from sedimentary to volcanic, particularly greenstones. The very low time terms associated with the greenstones and the systematic way in which the time terms decrease approaching the Sargent Fault suggest that the *Pg* refractor does indeed correspond to a horizon in the Franciscan which is rich in volcanic rocks, perhaps grading with depth into basaltic crust or the "basaltic substratum" suggested by Bailey *et al.* (1964); furthermore, it suggests that in this region the basaltic crust is relatively close to the surface. Alternatively, the low time terms might result from a local accumulation of volcanic material within the Franciscan. However, unusually small time terms are not associated with the large field of Miocene volcanic rocks east of Hollister.

Additional support for the association of the *Pg* refractor with a basaltic crust at the bottom of the Franciscan Formation comes from the relatively small time term located on the sliver between the San Andreas and Pilarcitos Faults. The sliver is composed of Franciscan material rich in volcanic rocks. At the southern end of the sliver, the Franciscan rocks are covered with Eocene sedimentary rocks. The time term of 0.4 sec is anomalously low for a station on Tertiary rocks, thereby suggesting a shallow *Pg* refractor. To the northwest, the sliver of Franciscan material rich in volcanics continues out to sea for an unknown extent. It is possible that this shallow, high-velocity material is responsible for the anomalously early arrival recorded by Healy (1963) in Golden Gate Park in San Francisco. This arrival, recorded 35 km northeast of the off-shore shot point, was almost 1 sec early relative to an arrival 25 km directly east of the shot point.

The large thicknesses of Tertiary rocks between the Sargent and San Andreas faults and to the south in the Hollister Trough are reflected in the large time terms. Studies of well data and surface structural relations suggest thicknesses of Tertiary sediment exceeding 3 km (Christensen and Knight, 1964b; Payne, 1967).

Southwest of the San Andreas Fault. The time terms in the area bounded by the Ben Lomond-Zayante (BL.-Z.), San Gregorio (S.G.), Pilarcitos (P.) and San Andreas (S.A.) faults (Figure 4) in the northern Santa Cruz Mountains are all between 0.6 and 0.8 sec. Travel times for distances less than 20 km suggest that the average velocity in the rocks above the *Pg* refractor is about 4 km/sec. Using this average velocity and a *Pg* refractor velocity of 5.9 km/sec, the depth to the *Pg* refractor (presumably granite basement) would be 3.3 to 4.4 km. This range of depth is in good agreement with geological estimates of depth to basement. Several wells in the area, drilled to a depth of the order of 2 km, failed to reach basement. The structural relations and stratigraphy determined by Cummings *et al.* (1962), together with the well data, suggest that the maximum depth to basement is in the central part of this area, and is at least 4.5 km.

Immediately south of the Ben Lomond and Zayante faults in the southern Santa Cruz Mountains, time terms ranging from 0.2 to 0.6 sec are obtained. Granite is exposed throughout much of this area. The small time terms indicate a shallow refractor below the surface of the granite.

Large time terms in the range 0.8 to 1.1 sec are obtained in the area bounded by a curve connecting the Ben Lomond, Zayante and Vergeles faults on the west and the San Andreas Fault on the east. The density of data is not sufficient to resolve the western boundary of this region of large time terms, but a few smaller time terms along the western periphery suggest that the basement offset along the Zayante Fault continues to the southeast, beyond the surficial exposure of the fault, in a narrow but rather deep trough filled

with sedimentary rocks. This inference is supported by the presence of a gravity low over this area (Chapman and Bishop, 1968; Bishop and Chapman, 1967; Clark and Reitman, 1971). The deepest well in the area bottoms in a Miocene sandstone unit at a depth of about 2.3 km (Christensen and Knight, 1964b). Stratigraphic and structural relations suggest that the basement may be as much as 1 km or more below the bottom

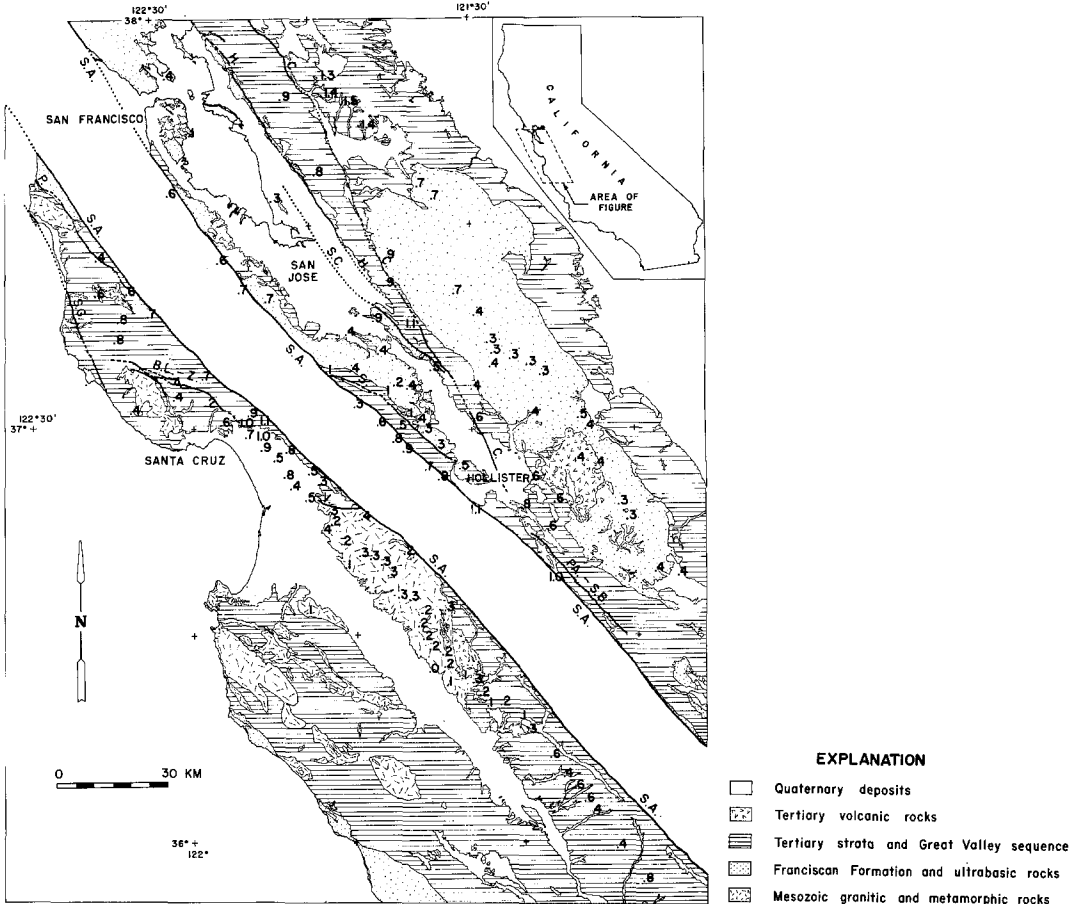


FIG. 4. Time terms (in sec) plotted on generalized geological map split along San Andreas Fault to show detail. The region southwest of the fault is translated directly westward relative to the region northeast of the fault. Letters indicate major faults: B.L.-Z., Ben Lomond and Zayante; C., Calaveras; H., Hayward; P., Pilarcitos; PA.-S.B., Paicines and San Benito; S., Sargent; S.A., San Andreas; S.C., Silver Creek; S.G., San Gregorio; and V., Vergeles. Geology is generalized after Jennings and Burnett (1961), Jennings and Strand (1958), and Rogers (1966).

of the well, yielding an estimated thickness of sedimentary rocks of 3 to 3.5 km, as compared with an estimated 4.4 to 6.1 km based on the time terms assuming an average velocity above the refractor of 4 km/sec. If the near-surface velocity should be lower than 4.0 km/sec, the calculated thickness would be reduced. The small time terms for sites on the San Andreas Fault just north of the Vergeles Fault may result from these stations being on granite, presumably, faulted slivers.

Within the Gabilan Range, the time terms are all in the range 0.0 to 0.4 sec, indicating a relatively shallow *Pg* refractor. Because granite is exposed throughout the Gabilan Range, it is clear that the *Pg* refractor does not correspond to the top of the granite.

It might seem paradoxical that in areas where the basement is covered with a thick section of sedimentary rocks, the P_g refractor is identified with the top of the granite basement, whereas in areas where granite is exposed at the surface, it is clear that the P_g refractor is clearly as much as 2.5 km below the surface. The explanation is quite straightforward. Velocity is not only a function of rock type and of physical properties, but it can also be a function of pressure and degree of fluid saturation. The increase of velocity with pressure is substantial for pressures below about 2 kb, corresponding to the lithostatic pressure at a depth of 7 to 8 km, but rather slight at larger pressures (Press, 1966). Because the lithostatic pressure at depth depends only on the density and thickness of the overburden and because the densities of both sedimentary and granitic rocks are in the same general range, the pressure at the bottom of a column of sedimentary rocks will be of the same order as that at the bottom of a column of granitic rock of comparable thickness. Therefore, whereas granite at the surface might have a velocity below 5 km/sec, the same rock buried beneath 3 to 5 km of sedimentary rocks would have a velocity of about 6 km/sec.

The effect of water saturation on seismic velocity, as described by Nur and Simmons (1969), might also explain the apparent discrepancy between 4 to 5 km/sec velocities observed near the surface and the 6.0 km/sec velocity at a depth of 2 to 3 km. This increase in velocity could correspond to the increase in the degree of water saturation associated with the water table. It is probable in this case, however, that the water table is within a few tens of meters of the surface.

Subdivision of data southwest of the San Andreas Fault. To check the consistency of the time-term analysis, the observations for the southwest side of the San Andreas Fault were divided into a north and a south group, roughly at the northern terminus of the Gabilan Range, and time terms for the two groups were calculated separately (Figure 5). The recalculation resulted in minor changes in the time terms (see Tables 4 and 5); however, the free solution refractor velocity for the northern area decreased substantially, from 5.9 to 5.6 km/sec. The smaller velocity change for the southern group, from 5.9 to 6.0, resulted from the bias in the average caused by the larger amount of data from the southern area. Despite the improved statistical appearance of the calculations, their significance in terms of geological reality is uncertain. The disparity between the refractor

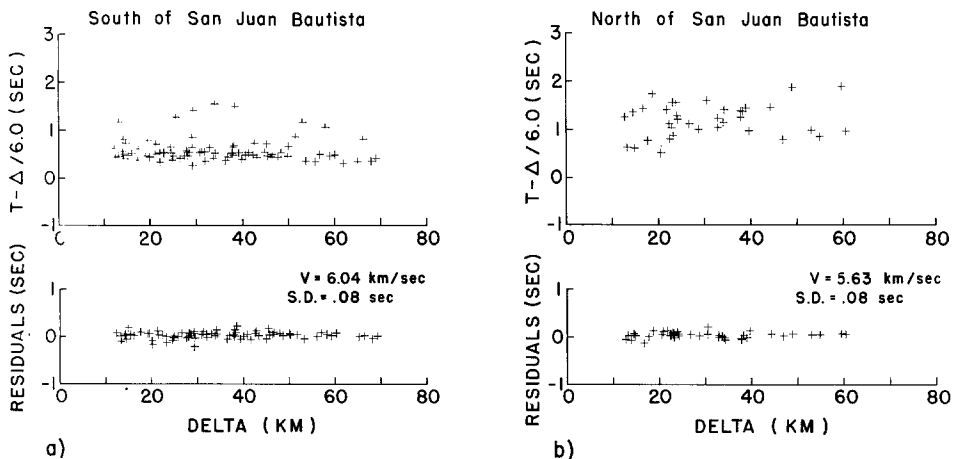


FIG. 5. Travel-time data and residuals plotted as a function of distance for subdivisions of the region southwest of the San Andreas Fault: (a) south of San Juan Bautista, and (b) north of San Juan Bautista.

velocities in the northern and southern areas is disturbing since surficial exposure, the few available drill holes, and the composition of the overlying sediments all support a granitic basement throughout the whole area (E. E. Brabb, oral communication, 1971). The low velocity obtained for the northern part of the area, lower than that expected for granitic rocks, is, therefore, troublesome. Assuming that these arrivals correspond to granite, the decrease in velocity in the northern area must result from either (1) a granite that differs in composition or physical properties or (2) a systematic error in the time-term method when applied to this geological structure. A structure and recording situation that would result in an anomalously low estimate of the velocity is illustrated in Figure 6. Shots on the margins of a sedimentary basin are not recorded at distances that completely span the basin, and the time-term method would systematically underestimate the refractor velocity because "down-dip" readings would predominate. Classical refraction profile interpretation techniques would have the same drawback. Most of the sources

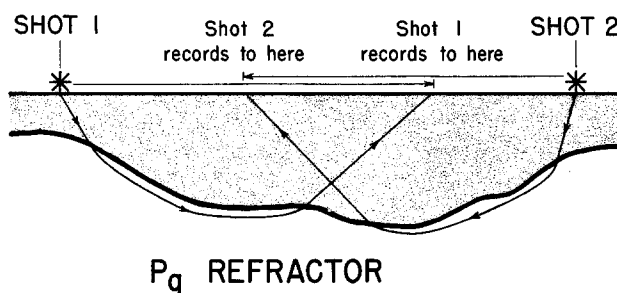


FIG. 6. Basement geometry that could result in underestimating refractor velocity. If arrivals from shot points on basement highs are not recorded all the way across the intervening lows, then the estimate of refractor velocity will be biased by a preponderance of "down-dip" observations and the estimate will be lower than the true value.

in the northern area, including Q03, Q04, Q10 and BBN2, were located on basement highs; therefore, it is possible that the anomalously low refractor velocity, as computed for the northern region, results from an inappropriate application of the time-term method.

Effect of topography. Assuming that the elevation of the refractor is independent of the surface topography, a positive correlation of large time terms with stations at high elevations is expected but is rarely observed. Normally, this is so because few stations are situated within an area of geological homogeneity. In fact, because of inhomogeneity, a negative correlation is often observed, with large delays in low valleys filled with low-velocity, unconsolidated sediments, and small delays in mountains composed of basement rock. However, sufficient data exist in the Gabilan Range to demonstrate a positive correlation, as shown by the plot of time term in relation to elevation (Figure 7). Only stations on granite or very near granite outcrops are considered. Time terms are plotted for both the complete southwest solution and the Gabilan solution alone. Some substantial differences are observed, but the trend was not substantially affected. This analysis is based on data from both the north and the south and the residuals (Figures 2a and 3) are not distance-dependent; therefore, it seems unlikely that the solution is biased. Since Figure 7 is, in a sense, a plot of travel time in relation to vertical distance, assuming a flat refractor, the observed trend may be used to calculate a vertical phase velocity of about 3.8 km/sec, from which the true intrinsic velocity, c , of the material

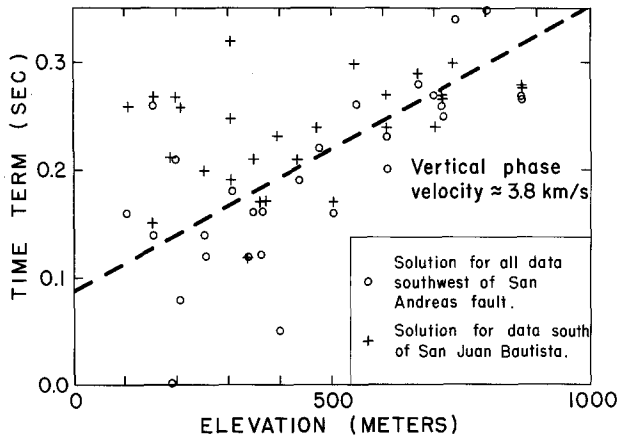


FIG. 7. Time terms for stations in the Gabilan Range as a function of station elevation.

may be calculated from the vertical and horizontal phase velocities, c_v and c_h , by the relation

$$c^{-2} = c_v^{-2} + c_h^{-2}.$$

The horizontal phase velocity is the slope of an ordinary travel-time curve or, in this case, the refractor velocity from the time-term solution, about 6.0 km/sec. This relation yields 3.2 km/sec for the material velocity, which is somewhat less than the near-surface velocity of 4.8 km/sec obtained by Stewart (1968). Nonetheless, the low value may reflect the velocity of the very near surface.

CONCLUSION

The correlation between the time terms obtained in this study and mapped geological structure is striking. The quality of the correlation assures that station corrections based on these time terms are based on geological reality. Favorable results in the interpretation of travel-time data for such a structurally complex area as the upper crust in central California support the reliability of such interpretations for certain regions, the lower crust, for example, where geological data are more ambiguous. It is clear that the enigmatic lower crust plays a very important role in tectonic processes, and details of its structure are vitally needed.

Perhaps, most importantly, the quality of the results obtained in this study demonstrates the potential for studying crustal structure, using a large seismic array combined with a seismic refraction program. Earthquakes accurately located using a calibrated array offer three enormous advantages over artificial explosions: larger size, greater depth, and generation of S waves. Once the velocity structure of the upper crust is sufficiently understood so that very accurate hypocentral coordinates for earthquakes can be obtained, earthquakes can be used as a very powerful tool in the study of crustal structure.

ACKNOWLEDGMENTS

The authors would like to thank the following quarry operators for permitting the U.S. Geological Survey to time their quarry blasts and for keeping us informed of especially large blasts: Piazza Paving Company, Kaiser Aluminum Company, Granite Rock Company, Kaiser Cement and Gypsum Corpora-

tion, Pacific Concrete and Aggregate, Ideal Cement Company, Kaiser Sand and Gravel, Quarry Products Inc., and Basalt Rock Company.

We are especially indebted to Mr. Ralph Hoffman, Mr. Ted Baldwin, Mr. Jack Lucas, Mr. Ed Baumgardner, and Mr. Angello Camello of the Kaiser Cement and Gypsum Corporation.

We would also like to thank many of our colleagues in the U.S. Geological Survey for their discussions of the geology and crustal structure of this region, particularly R. D. Brown, Jr., S. W. Stewart, R. M. Hamilton, J. H. Healy and J. P. Eaton who read the manuscript and suggested improvements. Research was carried out while one of the authors (R. L. Wesson) was pursuing an NRC-USGS Post-Doctoral Research Associateship. The work was done in cooperation with the Division of Reactor Development and Technology, U.S. Atomic Energy Commission.

REFERENCES

- Bailey, E. H., W. P. Irwin, and D. L. Jones (1964). Franciscan and related rocks, and their significance in the geology of western California, *Calif. Div. Mines Geol. Bull.* **183**, 177.
- Berry, M. J. and G. F. West (1966a). An interpretation of first-arrival data of the Lake Superior experiment by the time-term method, *Bull. Seism. Soc. Am.* **56**, 141-181.
- Berry, M. J. and G. F. West (1966b). A time-term interpretation of the first-arrival data of the 1963 Lake Superior experiment, *Am. Geophys. Union Monograph* **10**, 166-180.
- Bishop, C. C. and R. H. Chapman (1967). Bouguer gravity map of California, *Santa Cruz Sheet*, California Division of Mines and Geology, Scale, 1:250,000.
- Byerly, P. (1939). Near earthquakes in central California, *Bull. Seism. Soc. Am.* **29**, 427-462.
- Chapman, R. H. and C. C. Bishop (1968). Bouguer gravity map of California, *San Francisco Sheet*, California Division of Mines and Geology, Scale, 1:250,000.
- Christensen, E. W. and R. L. Knight (Compilers) (1964a). San Andreas fault cross section, Gulf of the Farrallones to Bielwaski Mountain, California, *Am. Assoc. Petroleum Geologists, Pacific Sect.*, Cross Section No. 2.
- Christensen, E. W. and R. L. Knight, (Compilers) (1964b). San Andreas fault cross section, Bielwaski Mountain to Hollister, California, *Am. Assoc. Petroleum Geologists, Pacific Sect.* Cross Section No. 3.
- Clark, J. C. and J. D. Reitman (1971). Preliminary geologic and gravity maps of Santa Cruz-San Juan Bautista area, Santa Cruz, Santa Clara, Monterey and San Benito Counties, California, *U.S. Geological Survey Open-File Map*, Scale, 1:125,000.
- Cummings, J. C., R. M. Touring, and E. E. Brabb (1962). Geology of northern Santa Cruz Mountains, California, in *Geologic Guide to Gas and Oil Fields of Northern California*, O. E. Bowen, Jr., Editor, *Calif. Div. Mines Geol. Bull.* **181**, 179-220.
- Eaton, J. P. (1963). Crustal structure from San Francisco, California, to Eureka, Nevada; Seismic-refraction measurements, *J. Geophys. Res.* **68**, 5789-5806.
- Eaton, J. P., W. H. K. Lee, and L. C. Pakiser (1970). Use of microearthquakes in the study of the mechanics of earthquake generation along the San Andreas fault in central California, *Tectonophysics* **9**, 259-282.
- Hamilton, R. M. (1970). Time-term analysis of explosion data from the vicinity of the Borrego Mountain, California, earthquake of April 9, 1968, *Bull. Seism. Soc. Am.* **60**, 367-381.
- Hamilton, R. M., A. Ryall, and E. Berg (1964). Crustal structure southwest of the San Andreas Fault from quarry blasts, *Bull. Seism. Soc. Am.* **54**, 67-77.
- Healy, J. H. (1963). Crustal structure along the coast of California from seismic-refraction measurements, *J. Geophys. Res.* **68**, 5777-5787.
- Jennings, C. W. and J. L. Burnett (Compilers) (1961). *Geologic Map of California, San Francisco Sheet*, California Div. Mines and Geology, Scale, 1:250,000.
- Jennings, C. W. and R. G. Strand (Compilers) (1958). *Geologic Map of California, Santa Cruz Sheet*, California Division of Mines and Geology, Scale, 1:250,000.
- Kind, R. (1972). Residuals and velocities of P_n waves recorded by the San Andreas seismograph network, *Bull. Seism. Soc. Am.* **62**, 85-100.
- McEvelly, T. V. (1966). Crustal structure estimation within a large scale array, *Geophys. J.* **11**, 13-17.
- Mikumo, T. (1965). Crustal structure in central California in relation to the Sierra Nevada, *Bull. Seism. Soc. Am.* **55**, 65-83.
- Nur, A. and G. Simmons (1969). The effect of saturation on velocity in low porosity rocks, *Earth and Planetary Science Letters*, **7**, 183-193.
- Otsuka, M. (1966a). Azimuth and slowness anomalies of seismic waves measured on the central California seismic array, Part I, Observations, *Bull. Seism. Soc. Am.* **56**, 223-239.

- Otsuka, M. (1966b). Azimuth and slowness anomalies of seismic waves measured on the central California seismic array, Part II, Interpretation, *Bull. Seism. Soc. Am.* **56**, 655-675.
- Page, B. M. (1966). Geology of the coast ranges of California, in *Geology of Northern California*, E. H. Bailey, Editor, *Calif. Div. Mines Geol. Bull.* **190**, 255-276.
- Payne, M. B. (Editor) (1967). San Andreas fault cross sections, east and west longitudinal cross sections parallel to the San Andreas fault and east to west cross sections across the San Andreas fault, California, *Am. Assoc. Petrol. Geologists, Pacific Sect.*
- Press, F. (1966). Seismic velocities, *Handbook of Physical Constants*, S. P. Clark, Editor, *Geol. Soc. Am. Mem.* **97**, 195-218.
- Raitt, R. W. (1963). The crustal rocks, in *The Sea, Vol. III*, M. N. Hill, Editor, Interscience Publishers, New York, 85-102.
- Robbins, S. L. (1971). Gravity and magnetic data in the vicinity of the Calaveras, Hayward, and Silver Creek faults, *U.S. Geol. Surv. Profess. Papers* **750-B**, B128-B139.
- Rogers, T. H. (Compilers) (1966). *Geologic Map of California, San Jose Sheet*, California Division of Mines and Geology, Scale, 1:250,000.
- Scheidegger, A. E. and P. L. Willmore (1957). The use of a least-squares method for the interpretation of data from seismic surveys, *Geophysics* **22**, 9-22.
- Shor, G. G., Jr., P. Dehlinger, H. K. Kirk, and W. S. French (1968). Seismic refraction studies of Oregon and northern California, *J. Geophys. Res.* **73**, 2175-2194.
- Stewart, S. W. (1968). Preliminary comparison of seismic traveltimes and inferred crustal structure adjacent to the San Andreas fault in the Diablo and Gabilan Ranges of central California, in *Proceedings of Conference on Geologic Problems of the San Andreas Fault System*, W. R. Dickenson and A. Grantz, Editors, *Stanford Univ. Publ., Univ. Ser., Geol. Sci.* **11**, 218-230.
- Turcotte, F. T. (1964). Epicenters and focal depths in the Hollister region of central California, *Ph.D. Thesis*, University of California, Berkeley, 124 pp.
- Willmore, P. L. and A. M. Bancroft (1960). The time-term approach to refraction seismology, *Geophys. J.* **3**, 419-432.

NATIONAL CENTER FOR EARTHQUAKE RESEARCH
U.S. GEOLOGICAL SURVEY
MENLO PARK, CALIFORNIA 94025

Manuscript received February 8, 1973